UNIVERSITÀ DI GENOVA

DOCTORAL THESIS

Como Hacer un Asado

Author:
Pedro LAGOMARSINO DE LEON ROIG

Supervisor:
Dr. Tommaso FELLIN

January 4, 2021

Abstract of thesis entitled

Como Hacer un Asado

Submitted by

Pedro LAGOMARSINO DE LEON ROIG

for the degree of Doctor of Philosophy

at The Università di Genova

in January, 2021

Put Your *Abstract* Here ...

This latex project is a doctoral thesis template for the University of Hong Kong. The style and design of the entire project closely follow the official guidelines from the Graduate School: **Preparing and Submitting Your Thesis — A Guide for MPhil and PhD Students.** Generally, there is no strict stipulations on the style or format of different components of the thesis, except for the **Abstract**. According to the detailed regulations [**Link**], the **Abstract** should be part of the thesis with no fewer than 200 and no more than 500 words. The format shall be the same as that of the thesis itself. The front page of each abstract shall contain the statement which includes:

- Abstract of thesis entitled "……"
- Submitted by ……
- for the degree of ……
- at the Università di Genova in (January 4, 2021).

In addition to the opening of abstract, the abstract should appear before the title page. The abstract in this template is not numbered, or counted in the pagination of the front matter, or listed in the table of contents. All the requirements are fulfilled in this template.

How to adjust the typeset of Abstract

The typeset of the opening of abstract page is defined in the class file HKUThesis.cls **Line 507-529**. Users can adjust the typeset by changing the settings. The layout of the main text is consistent with other parts of the thesis.

Note that: Considering the university may change its standards over time, users are not supposed to 100 percent "trust" this template. Even though the template is prepared strictly follow the stipulations of the Graduate School of The University of Hong Kong, this is **not an official** template and we are **not responsible** for any problems of your

thesis submission caused by the format, style, typeset, etc of the template. We **strongly suggest** the users to read the latest **Guidelines on Thesis Submission** carefully and adjust the template accordingly to satisfy the stipulations of the university.

Como Hacer un Asado

by

Pedro LAGOMARSINO DE LEON ROIG
B.S. *UNIGE* M.S. *UNIGE*

A Thesis Submitted in Partial Fulfilment
of the Requirements for the Degree of
Doctor of Philosophy

at

Università di Genova
January, 2021

For Mama and Papa

Acknowledgements

I would like to thank...

Pedro LAGOMARSINO DE LEON ROIG
University of Hong Kong
January 4, 2021

Contents

List of Figures

List of Algorithms

List of Abbreviations

mEC	**m**edial **E**ntorhinal **C**ortex
CNS	**C**entral **N**ervous **S**ystem
FOV	**F**ield **O**f **V**iew
DLC	**D**eep **L**ab **C**ut
CNN	**C**onvolutional **N**eural **N**etwork
MSE	**M**ean **S**quare **E**rror
ROI	**R**egion **O**f **I**nterest
AP	**A**ction **P**otential
VR	**V**irtual **R**eality

List of Symbols

Global notations

I^{SR}	super-resolved light field image	—
I^{LR}	low-resolution light field image	—
I^{HR}	high-resolution light field image	—
E^{SR}	super-resolved epipolar plane image	—
E^{HR}	high-resolution epipolar plane image	—

Chapter 1

θ, ϕ	incoming direction expressed in term of spherical coordinates	rad
τ	time	s (second)
x,y	spatial coordinates with two-plane parameterization	1 (uint)
s,t	angular coordinates with two-plane parameterization	1 (uint)
P	radiance distribution	$\mathrm{W/srm^2Hz}$
Ω	image plane	—
Θ	parameters of the multi-layer framework	—
γ_s, γ_a	scaling factors of spatial / angular coordinates	1 (uint)
$\mathcal{L}$	loss function	—

Chapter 2

F_0	shallow features extracted by a single HConv layer	—
$F_{\mathrm{G_d}}$	feature maps extracted by the d^{th} HRB of the GRLNet	—
$H^{\mathrm{n}}_{\mathrm{HRB}}$	the operation of the n^{th} HRB of the SReNet	—
H_{AGBN}	the operation of the proposed aperture group batch normalization algorithm	—
H_{up}	upsampling operation on the low-resolution features	—
ℓ_A	angular loss	—
ℓ_S	spatial perceptual loss	—
ℓ_{SA}	the weighted combination of ℓ_A and ℓ_S	—

f	the summation of all the feature maps after every activation function of VGG network	—
g	learned mapping between the low-resolution and high-resolution light field images	—

Chapter 3

x,y	spatial coordinates with two-plane parameterization	1 (uint)
s,t	angular coordinates with two-plane parameterization	1 (uint)
γ_s, γ_a	scaling factors of spatial / angular coordinates	1 (uint)
ℓ_G	generator adversarial loss	—
ϕ	denotes the mapping of VGG network	—
δ	nearest neighbor downsampling operator	—
κ	a Gaussian blurring kernel with a window size of 7×7 and standard deviation of 1.2 pixels	—
η	additive noise with zero mean and unit standard deviation	—

Chapter 1

Introduction

1.1 Spatial navigation

The interaction between organisms and the environment is the core of life and evolution. This interaction happens at different levels with different objectives and outcomes. From the behavioural point of view, organisms have evolved to be able to perceive different aspects of the environment, interpret them and act in consequence. The more we move forward in evolution the more sophisticated and complex resources and behaviours we observe, being the nervous system, perhaps, the mayor and most interesting exponent of this.

One of the most fundamental aspects of such interaction consists on being able to move and navigate through the environment. A functional navigation system has to achieve a series of very difficult tasks that include the integration of information from different sensory modalities and coordination with the motor system, together with higher order cognitive processes like proprioception and goal directed activity in a flexible and dynamic way.

Spatial navigation has been extensively studied in the last 50 years, in particular, in the mammalian brain. The seminal work of John O'Keefe during the 1970s on rats lead to the hypothesis of a *cognitive map* [O'Keefe and Nadel, 1980] as the way the brain solves the challenge of spatial navigation and, importantly, to experimental corroborations of the possible neuronal implementation of it. Unexpectedly such implementation involved the activity of specialized cells in a restricted area of the brain: **The Hippocampus**.

According to the *cognitive map* theory, cells in the Hippocampus would receive inputs conveying information about sensory cues related to environmental stimuli, calculate the animal's position in space and consequently predict subsequent positions and trajectories depending on goal, inferred distances and directions. The ability of the internal navigation system to calculate trajectories and predict future positions represents the essence of learning in the cognitive map and has several implications regarding the internal structure, what kind of computations and types of cells should be find in the Hippocampus.

In the next sections we will summarize the anatomy and function of the Hippocampus and the different types of information encoding cells found to be present in the hippocampal navigation system.

1.1.1 The Hippocampus

Although hippocampal anatomy and connectivity has been extensively studied for decades, it's understanding and it's relationship with function is far from being completely elucidated [reference to something about discrepancies or open questions]. Here we will briefly described the canonical hippocampal circuit, it's constituents, structure and connectivity, paying special attention to the flow of information in the circuit.

The mammal Hippocampus is a seahorse-shaped (hence the name) brain structure located underneath the temporal lobe of the neocortex. All mammals have a structure that could be identify as an Hippocampus, moreover, it is possible to identify a homologue of the mammalian hippocampus in all vertebrates [O'Keefe and Nadel, 1980, Kappers, Huber, and Crosby, 1936, Heier, 1948, Crosby, DeJonge, and Schneider, 1966]. It's interesting to note though, that besides the difference in structure, the Hippocampus homologues can play an entire different functional role. The grid like structure of the Hippocampus could be thought as a general mapping structure that accomplish different functions depeneding on the species. In the mouse and rat, which is the case that concerns this work, is thought to be used as a spatial mapping structure, as discussed before.

In this animal the Hippocampus occupies a large portion of the forebrain and represents the paradigm of the simple cortex, consisting primarily of one basic cell type, the pyramidal or granule cells, and its asociated interneurons, the basket cells [Figure 1.1b]. In fact, a horizontal section through the posterior arch of the hippocampus shows the transition form the six layered complex structure of the entorhinal neocortex to the three layered hippocampal formation through the *subiculum* [Figure 1.1a].

The hippocampal structure can be divided in two U-shaped interlocking sectors, the *hippocampus proper* and the *dentate gyrus*. The hippocampus proper can, in turn, be divided in 4 subfields CA1-4 [Lorente De Nó, 1934]. CA stands for *cornu ammonis*, another shape-like reference. Following the structured layer of principal neurons, CA1 appears first as the main output region of the hippocampus, followed by CA2-3 in the regio inferior and finally CA4 represents the scattered cells inside the hilus of the dentate gyrus [see Figure 1.1a]. With the exception of CA4, all regions of the hippocampus have a common simple structure: a compact and dense layer of cell bodies who's dendrites stretch in the same direction and receive most of their inputs from perpendicular running axons that make synapsis with many neurons at constrain regions of the dendrites. Such simple and preserved structure of the hippocampus represents one of the key aspects of it's function. The different subregions differ in the types of cells they have, CA3 having giant pyramids, CA1 smaller pyramids and granule cells in the dentate gyrus.

Internally the dentate gyrus has three layers [Figure 1.1b right]: the *granule* layer that contains the cell bodies of the mentioned granule cells, the *molecular* layer consisting of the apical dendrites of the granule cells and their afferents and finally the *polymorph* layer in the concave hilus of the dentate gyrus formed by the axons of the granule cells. This axons later conform the mossy fiber bundle that merges with CA4. Present in this last layer there're also some scattered basket cells interneurons. The hippocampus proper, although it's basically a three layered structure, it can be further divided for better describing the pyramidal cells and their afferents [Figure 1.1b left]. First there's the *alveus* layer formed by the axons of the pyramidal cells that project to the subiculum, then we find the *stratum oriens* containing the basal dendrites, some basket cells and afferents from the septum. Third, the *stratum pyramidale* with the cell bodies and finally the *stratum radiatum* and the *stratum moleculare* with different parts of the apical dendrites. It's interesting to note that the main feature conveying the lamination of the hippocampal structure is the nature of their afferents, briefly described next.

The connectivity in the hippocampus is highly complex and the afferents arise from many different regions of the brain, here we will describe only the canonical circuit [Figure 1.1a], starting with the **extrinsic afferents**. The main source of input to the hippocampus is the entorhinal cortex that projects from its lateral and medial regions, passing by the upper layers of the subiculum, to either the hippocampus proper through the perforant path or to the dentate gyrus through the hippocampal fisure [Nafstad, 1967, Hjorth-Simonsen and Jeune, 1972, Van Hoesen, Pandya, and Butters, 1972, Hjorth-Simonsen, 1973, Van Hoesen and Pandya, 1975].

Once in the hippocampus the major **interconnections between sectors** are primarily unidirectional, starting from the dentate gyrus, through CA3 and ending in CA1 [Lorente De Nó, 1934, Raisman, Cowan, and Powell, 1965, Hjorth-Simonsen, 1973, Andersen, Blackstad, and Lomo, 1966, Fujita and Sakata, 1962, Gloor, Vera, and Sperti, 1963]. Cells in the dentate gyrus have axons that gather together in the hilus forming the mossy fibers. The mossy fibers split in two bundles that project to the hippocampus proper. One bellow the pyramidal neurons in the stratum oriens, that stops abruptly in CA3. The second bundle runs above the pyramidal cells of CA3 through the stratum lucidum and continues until the border of CA1. CA3 and CA4 neurons make powerfull excitatory connections to the stratum radiatum of CA1 called *shaffer collaterals* [Lorente De Nó, 1934, Hjorth-Simonsen, 1973, Andersen, Blackstad, and Lomo, 1966]. Collaterals from CA3 and CA4, potentially the same that form the *shaffer collaterals*, bend and project back to the proximal dendrites of the granule cells in the dentate gyrus [Zimmer, 1971]. It is believed that CA1 does not project back to CA3 [Raisman, Cowan, and Powell, 1966, Hjorth-Simonsen, 1973] but it is unclear if it projects to the dentate gyrus [Hjorth-Simonsen, 1973]. Interestingly CA1 and the dentate gyrus receive inputs from CA3 of both hippocampi, including the contralateral one. Then the information flows out of the hippocampus by CA1 cells axons that project to the septum and to the subiculum which in turn projects back to the entorhinal cortex, closing the loop in the

information flow [a schematic of this connection can be seen in Figure 1.1a].

Finaly, there's the **intrinsic afferents from the same sector,** that is, within each region of the hippocampus there's local connectivity in two flavours, excitatory monosynaptic connections between close by pyramidal neurons [Lebovitz, Dichter, and Spencer, 1971] and inhibitory polysynaptic connections due to the instrinsic pyramidal - interneuron - pyramidal loops, where the interneurons are the basket cells mentioned before [Kandel, Spencer, and Brinley, 1961, Spencer and Kandel, 1961, Andersen, Eccles, and Loyning, 1964a, Andersen, Eccles, and Loyning, 1964b].

To complete this brief description of the calssical hippocampal circuit we have to mention that the entorhinal cortex in turn receives a plethora of inputs from different parts of the brain, among which there are the prefrontal and cingulate cortices [Adey, 1951, Adey and Meyer, 1952, White, 1959, Cragg, 1965, Raisman, Cowan, and Powell, 1965, McLardy, 1971, Leichnetz and Astruc, 1975], the temporal cortex [Cragg, 1965], parietal areas [Pandya and Kupyers, 1969, Pandya and Vignolo, 1969, Petras, 1971], pyriform cortex [Powell, Cowan, and Raisman, 1965], the olfatory [Cragg, 1960, Cragg, 1961, Heimer, 1968, White, 1965, Price and Powell, 1971, Kerr and Dennis, 1972] and visual systems [Casey, Cuenod, and Maclean, 1965,Cuenod, Casey, and MACLEAN, 1965] and the amygdala [Krettek and Price, 1974].

This is by no means a full description of the hippocampal connectivity and its afferents, but only a succinct description of the canonical pathway through which information flows in the circuit. In this description information flows from several regions of the neocortex and other brain region to the entorhinal cortex and subiculum, from here to the dentate gyrus, then to CA3-4, finalizing in CA1 that projects back to the subiculum and entorhinal cortex (and to the septum) closing the loop. Interestingly, the projections in this path are topographically precise, in the sense that, for example, a small number of cells in the dentate gyrus projects to a small number of cells in CA3.

How does such a precise and well define anatomy and connectivity structure solve the problem of spatial navigation? When O'Keefe first elaborated the *cognitive map* theory he hypothesized that each of the three regions of the hippocampus accounted for a stage in the mapping system [O'Keefe and Nadel, 1980]. The first stage, occurring in the dentate gyrus, would consist in organizing the environmental inputs from the entorhinal cortex and subiculum into a schema required by the mapping system. This complex integrations would then be transmitted to CA3-4 where the second stage of the map would take place, by representing locations in an environment and the relationship between locations. Finally in CA1 the continuation of the map would be represented together with a mismatch system that would account for novelty or change in location information.

This very simple schematic turned out to be highly accurate in some senses and the last 4 decades of experiments have come up with empirical evidence of implementations of such system. The scheme has been improved and completed over the years, the current understanding in the field includes the subiculum and entorhinal cortex as

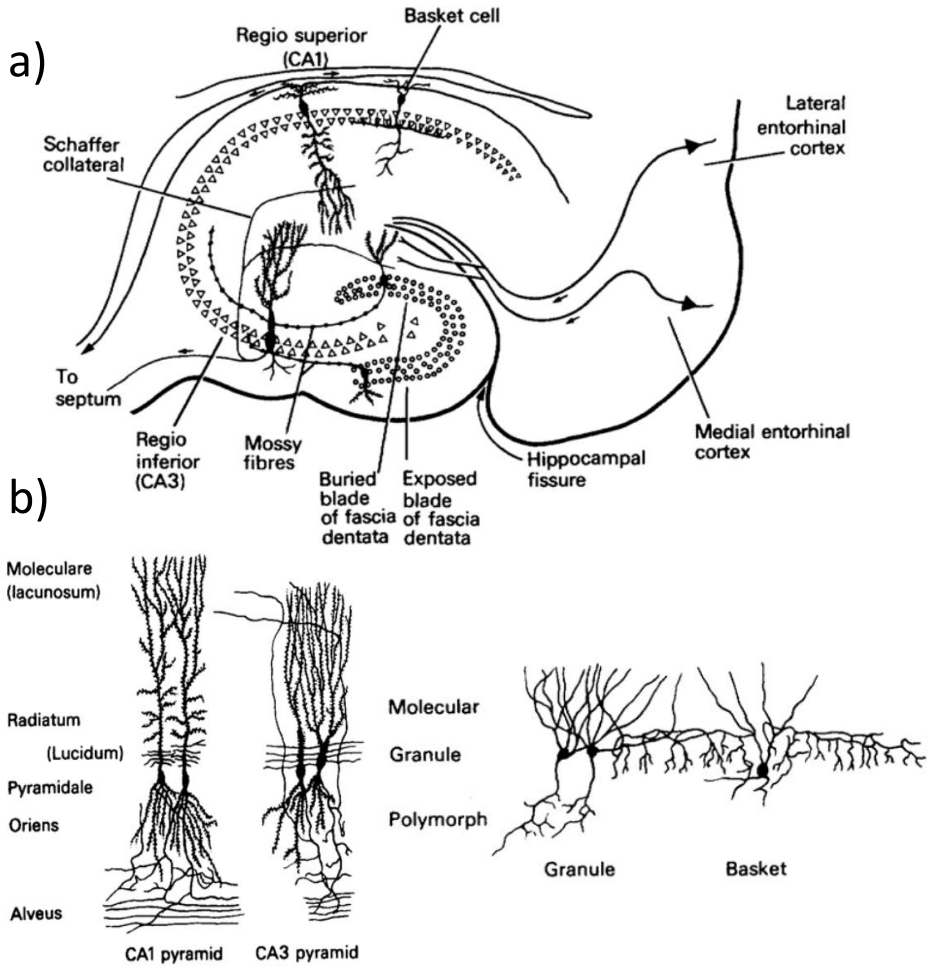

Figure 1.1: Hippocampal anatomy. a) Schematic representation of the mouse hippocampus and the connections between regions, adapted from [O'Keefe and Nadel, 1980]. b) Examples of CA1 and CA3 pyramidal cells (after Cajal 1911, Fig. 475) and of dentate granule and basket cells of Cajal (afterLorente De Nó, 1934, Fig.10).

part of the greater hippocampal formation. And in each of these regions it has been found a set of highly specialized neurons that together form the spatial map. Many of them have been predicted in the '70 by the *cognitive map* theory. According to it cells that encode position, distance and speed would be necessary. In the next section we'll summarize the main types of cells of the circuit and how they fit in the overall scheme.

1.1.2 Spatial information encoding cells

The first type of cells that conform the cognitive map were found by O'Keefe and Dostrovsky in 1971, when electrophisiological recordings in the hippocampus led to the discovery of cells that would fire predominantly in a specific location of a familiar environment [1.2a]. This cells were called *Place cells*. It's impossible to summarize here all what is currently known about place cells, so we will focus only in the main

characteristics of this and the rest of the cell types of the cognitive map.

Place cells are mainly found in the hippocampus proper and their firing rate is modulated purely by spatial location, that is, they fire maximally when the animal's head is in a specific region of the environment [Figure **??**a]. This region is called the *place field* of the cell [Figure **??**b]. Here we use the term environment in a generic way, but place cells have been mainly studied in constrained laboratory environments. Interestingly, place cells have different characteristics depending on the nature of the space the animal explores. Place cells fire at their place field location, regardless of directions of motion or speed when the animal is in a two-dimensional space, like the square/rectangular or circular boxes used in the early O'keefe experiments, but when exposed to a linear track, or one-dimensional environment, place cells would have a preferred direction of firing, and would fire much less or not at all or in a different location when the animal runs in the opposite direction [B. McNaughton, Barnes, and O'Keefe, 1983, O'Keefe and Recce, 1993]. Place cells have also been found in three-dimensional environments, having three-dimensional place fields. The latter type of place cell has been observed in bats flying through a familiar environment [Yartsev and Ulanovsky, 2013], and more recently in rodents exploring three-dimensional environments [R. Grieves et al., 2020].

The way place cells represent position is not limited to the firing rate of the cells but also to the temporal aspect of their firing. Place cell firing is locked to the phase of the sinusoidal local field potential (LFP), called theta rhythm, and hence to the population activity in the hippocampus. The theta rhythm works as a sort of clock against which the network can measure time and temporally locate cell spikes allowing place cells to identify locations in an environment with much finer precision than if only rate codes were used. This is called *Temporal coding* [O'Keefe and Recce, 1993, Huxter, Burgess, and O'Keefe, 2003, G. Buzsáki and Draguhn, 2004, G. Buzsáki, 2002].

Nearby place cells do not necessarily have nearby place fields, furthermore, a group of close by place cells would typically have place fields that span the whole space, suggesting that place cells represent a complete and highly redundant representation of the surface [O'Keefe, 1976, Wilson and B. L. McNaughton, 1994]. Once formed, these representations are stable across days [Hill, 1978, R. Muller, Kubie, and Ranck Jr., 1987] or even weeks [Thompson and Best, 1990]. Although, more recently, it has been suggested that not all place fields are stable [Mankin et al., 2015, Ziv et al., 2013].

There's a large portion of literature related to what are the necessary inputs to the hippocampus for a place cell to fire. This is still an unsolved question, although there are some clear hints. It is clear that visual information is important, as distal cues or landmarks surrounding the environment can influence place field formation [R. Muller and Kubie, 1987, O'Keefe and Conway, 1978, Yoganarasimha and Knierim, 2005] but it is not necessary. Place cells would fire in the same location in the dark in a familiar environment [Save, Nerad, and Poucet, 2000, Zhang et al., 2014, Markus, B. McNaughton, and Gladden, 1994, Quirk, R. Muller, and Kubie, 1990], provided that other sensory

cues are available such as olfaction or tactility. All this different modalities are integrated outside of the hippocampus [K. Jeffery, 2007], which shows that place fields are higher order representations that integrate more primitive spatial constructs such as direction, self motion and boundaries, which again talks about the inputs to the hippocampus. If the sensory cues show that the environment has changed or is completely new, a new and unique representation would be formed by the place cells [Anderson and K. Jeffery, 2003, O'Keefe and Conway, 1978] in a process called remapping [R. Muller and Kubie, 1987]. Importantly, in rats and mice, the animal has to explore the space directly for place cells to form a spatial representation [Rowland, Yanovich, and Kentros, 2011], unlike other mammals like primates that can form inferred allocentric representations of remote space if observed [Rolls, 1999, Rolls, Robertson, and Pierre, 1997, Rolls and O'Mara, 1995].

So far we've used a rather vague definition of place cell. Traditionally, to define a place cell and its place field several criteria related to the firing rate, consistency of firing or reliability were used. Here and throughout this work we will define a place cell as a cell in the hippocampus proper that carries *significant amount of information* about the animals position in it's firing activity (see methods). Later on we will define what this means in this context and how we establish significance.

The second key cell type in the spatial representation are the **head direction cells** [Figure 1.2d]. Head direction cells are cells in the presubiculum whose firing is modulated, as the name implies, by the facing direction of the head. They were first found by Rank [Ranck Jr., 1984, Ranck Jr., 1985] and described in detailed a few years later [Taube, R. J. Muller R., and J.B., 1990, Taube, R. Muller, et al., 1990, Taube, R. Muller, et al., 1987]. Here *head direction* refers to the orientation of the head in the horizontal plane. Head direction cells are very similar in their characteristics to place cells: they have a prefer direction of firing that is independent of other behavioural factors; each head direction cell has a different preferred direction; all together, preferred directions are equally distributed in the circle, in the sense that there's no overall preferred direction of the network [Taube, R. Muller, et al., 1990]. Like with place cells, angular orientation of environmental cues are an important modulator of head direction cells activity [figure 1.2d] [Goodridge and Taube, 1995, Taube, 1995, Taube, R. Muller, et al., 1990, Zugaro, Tabuchi, and Wiener, 2000, Knierim, H. Kudrimoti, and B. McNaughton, 1995] but are by no means necessary [Mizumori and J. Williams, 1993, Yoder, Clark, Brown, et al., 2011, Yoder, Clark, and Taube, 2011]. An interesting characteristic of this cells is that the angular relationship between preferred directions of different cells is preserved [Skaggs, Knierim, and B. Kudrimoti H. a., 1995, Yoganarasimha and Knierim, 2005]. Hence when remapping an environment or if the animal is disoriented and one cell changes its orientation, the rest of the cells change theirs coherently.

With place cells and head direction cells, the cognitive map is able to build positions and to measure angles. The next requirement for the map to work is a way of measuring distances, to establish the metric of the map. In 2005 a cell type that

could achieve this task was found in the Moser's lab: the **grid cells**. Grid cells are cells that fire in multiple discrete and regularly spaced locations which form a triangular or, equivalently, an hexagonal lattice [Figure 1.2c]. This cells are found in the medial entorhinal cortex (mEC) and postrhinal cortex [Fyhn, Molden, et al., 2004, Hafting et al., 2005, Fyhn, Solstad, and Hafting, 2008] and in the pre- and para-subiculum [Boccara et al., 2010].

Grid cells have some similar characteristics to place cells or head direction cells. Their pattern of firing arises in familiar environments and partially relies on distal visual cues; if the environmental cues rotate, grid patterns do so too consistently [Hafting et al., 2005]; and deformation of the environments implies deformation of he patterns [Barry, Hayman, et al., 2007, Stensola et al., 2012]. Like head direction cells, the angles and distances between grid patterns of different grid cells are preserved, and when the environment rotates or moves, the patterns adapt in a coherent fashion, mantaining a stable relationship [Fyhn, Hafting, et al., 2007]. This suggests that grid cells work cooperatively, as an interconected matrix known as attractor network [B. McNaughton, Battaglia, et al., 2006]. Moreover, the spacing between peaks of grid patterns varies as a function of location in the entorhinal cortex. The scales of the patterns increase in discrete jumps as one goes from dorsal to ventral in the entorhinal cortex [Brun et al., 2008]. Each animal can have 3 or 4 different scales.

Finally, we have the **boundary cells** [figure 1.2e left]. With yet another highly descriptive name, boundary cells, or boundary vector cells, are cells in the subiculum that respond purely to environmental boundaries [Figure **??**c top-right]. Interestingly, the existence of boundary cells was first hypothesized after the observation that after elongating one side of a rectangular box, place fields would stretch accordingly [O'Keefe and Burgess, 1996]. This led a number of researchers to think that there could exist cells that would fire in relation to environmental boundaries, and that place cells firing could arise as a thresholded sum of a subpopulation of such cells [Barry, Lever, et al., 2006, Burgess et al., 1997, Hartley et al., 2000]. Cells that fit such description, at least partially, were later found in several regions of the brain, like the subiculum [Barry, Lever, et al., 2006], presubiculum and parasubiculum [Boccara et al., 2010], mEC [Bjerknes, E. Moser, and M.-B. Moser, 2014, Savelli, Yoganarasimha, and Knierim, 2008, Solstad et al., 2008] and recently in the anterior claustrum [Jankowski and O'Mara, 2015] and rostral thalamus [Jankowski, Passecker, et al., 2015].

More formally we could define boundary vector cells as cells that fire when the animal encounters an environmental boundary in it's preferred direction. And it's firing is driven by the memory of the boundary's position related to the animal, based not only on perceptual cues, but also on self motion information [Lever et al., 2009, Raudies, Florian, et al., 2012, Raudies and Hasselmo, 2012]. This definition requires that we clarify two things: first, what is a boundary? A boundary can be walls, low ridges or vertical drops and the colour, texture or odour of these does not seem to influence the cell's firing [Lever et al., 2009]. Second, what does it mean to *encounter* a boundary?

Cells would fire at a specific distance from the boundaries, and this distance is different for cells in different brain regions [Bjerknes, E. Moser, and M.-B. Moser, 2014, Solstad et al., 2008, Jankowski, Passecker, et al., 2015, Lever et al., 2009].

Place cells, head direction cells, grid cells and boundary vector cells lie at the core of the cognitive map and represent the most relevant and more studied type of cells in the context of spatial navigation. However the further the cognitive map and the greater hippocampal formation is studied, the more *types* of cells are found. Cells with more abstract or complex firing patterns, cells that respond to clear real-world correlates, but also cells that respond to more abstract or conjunctive correlates. We will not describe them here, but in this list we should mention **object cells**, **goal cells**, **boundary-off cells**, **perimeter cells** and **band cells**, among others [figure 1.2e center and right].

It's interesting to think how each of this cell types can arise, due to which inputs, and in which combinations. In other words, what is the relation between the firing patterns of all these cell types? Mathematically is easy to show that place cells can be formed by summing two grids of different spacing, or equivalently by summing two border cells, or that grid cells can be built by combining band cells. The function and structure of each of this firing patterns is not yet understood. It is however almost difficult to believe that the brain builds such an explicit and interpretable map, using specialized cells in trackable combinations. This is of course, just the tip of the iceberg and the more the extended hippocampal formation is studied, the more cell types and complicated firing patterns appear.

1.1.3 Calcium as a proxy of spiking activity

With a few exceptions, the entirety of the research presented so far has relied on electrophysiological recordings of neuronal activity. Electrophysiology has long been the the preferred technique to interrogate brain activity, for historical reasons, but mainly because of its versatility, with exceptional temporal resolution and ability to integrate neuronal signals over wide scales, from individual APs to network oscillations [C. Buzsáki, Anastassiou, and Koch, 2012], intracellularly [Margrie et al., 2003] and extracellularly [Hubel and Wiesel, 1959]. In the last few decades, huge technological improvements in micro- and nano-fabrication techniques for multielectrode arrays [Bareket-Keren and Hanein, 2012,Spira and Hai, 2013,Viventi and Blanco, 2012,Jun, Steinmetz, and Siegle, 2017] helped solving several constrains of the technique, improving sampling density and biocompatibility. At the same time the development of modern analytical methods permitted the extraction of several types of information from this kind of recording [Agarwal et al., 2014, Shein-Idelson et al., 2017]. Electrophysiologial approaches have come a long way and continue to develop into a reliable and versatile way of studying neuronal activity, however it suffers from several limitations, such as a strong bias towards the detection of cells with high firing rate in unit recordings, invasiveness [Kim, McCall, and Jung, 2013], it's limited in terms of the study of correlation between

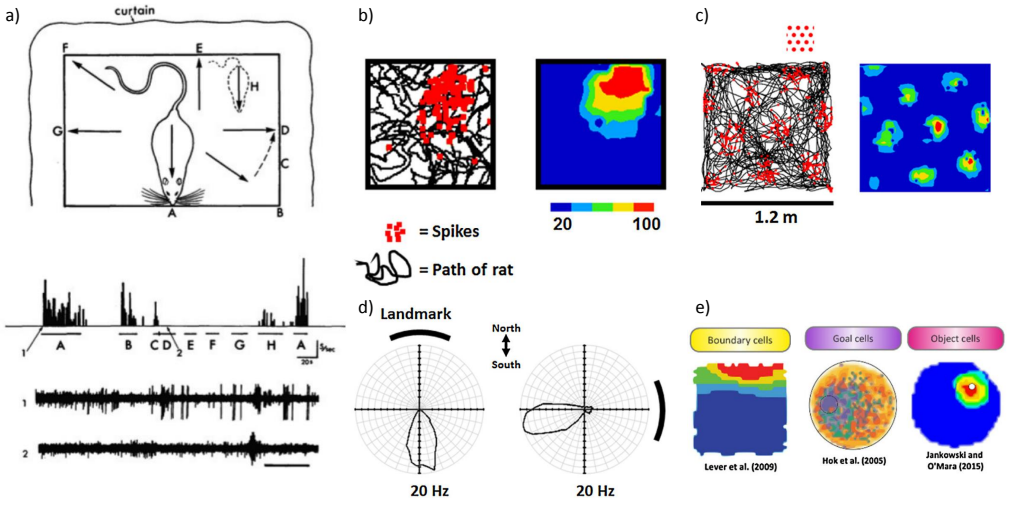

Figure 1.2: Spatial information encoding cells. a) The first report of a place cell in the hippocampus of the freely moving rat. The animal navigated a box (top). The cell fired only when the animal was in locations A and B. After O'Keefe and Dostrovsky (1971). b) Spikes (red squares) from a single hippocampal cell and path of the animal (black line) on a single trial (left), on the right the same data is shown as a heat plot of dwell-time-adjuted firing rate, between peak and 20% peak amplitude, this evidences the place field of the neuron. c) Grid, close-packed hexagonal firing pattern of a single entorhinal grid cell, firing depicted as in b). Characteristic distances from the lattice are specific to each cell and relatively constant in different environments, suggesting the encoding of distances. d) Two trials recorded from a post-subicular head direction cell, in a symmetrical environment having a single polarising landmark. Polar plots show firing rate as a function of the direction of the animals head. When the landmark is positioned north (left), the cell fires maximally when the animals's head faces south. When the landmark was rotated to the east (right, animal did was not present when change occur), the cell fires to the west, maintaining the equivalent relationship to the landmark. Showing that cells are influenced by local cues and not by geocentric ones such as the Earth's magnetic field. b), c) and d) adapted from R. M. Grieves and K. J. Jeffery, 2017. e) Examples of other types of navigation cells, references in place.

function and structure [D. A. Dombeck, Harvey, et al., 2010] and, importantly, the difficulty in distinguishing genetically selected neuronal populations. Alternative experimental methods partially overcome some of these limitations. Macro-scale imaging techniques, such as fMRI, are a remarkable example that had a strong impact in neuroscience, allowing the investigation of the involvement of spatially distributed neuronal circuits in response to external stimuli or in certain behavioral states, both in normal and pathological conditions [Craddock et al., 2013, Uğurbil et al., 2013, Van Essen et al., 2013]. This approaches, that are related to the hemodynamic response, have at the same time limitations in therms of temporal resolution and hardly give us information about activity at the cellular or subcellular scale. Alternatively, the last 3 decades came up with the development of optical imaging methods and fluorescent activity reporters that have provided an additional and efficient tool to study neural networks and their functions that overcomes some of the limitations of the methods described above [Ohki et al., 2005,Shoham et al., 1999, Grienberger and Konnerth, 2012, Bovetti, Moretti, and Fellin, 2014, Yang and Yuste, 2017]. Moreover, electrophysiology and Macro-scale imaging rely exclusively in the electrical activity of cells, which suites the study of neuronal networks accordingly, but prevents the observation of non-electrical activity of other cell types, like astrocytic calcium transients. The current success of such methods strongly rely on two technical advances: the synthesis of fluorescent calcium indicators and the development of non-linear microscopy, which made possible the recording of large ensembles of neurons with subcellular spatial resolution and adequate temporal resolution in intact tissue the activity [Bovetti, Moretti, and Fellin, 2014, Yang and Yuste, 2017, Svoboda and Yasuda, 2006].

Action Potential (AP) firing, as well as synaptic inputs, leads to the opening of voltage-gated calcium channels in neurons, which induce a transient elevation in cytoplasmic Ca^{2+} concentration. This variations are typically in the range of 50-100 nM to 5-10 μM and can be detected by the fluorescence calcium indicators. In this way, neurons stained with these compounds expose fluorescence changes in the soma after AP firing [Yuste and Katz, 1991]. Calcium transients are localized and decay over 100–500 ms, through diffusion, the activity of calcium extrusion mechanisms, and internal buffering molecules [Grienberger and Konnerth, 2012]. Importantly, electrical excitability is not necessary condition for calcium excitability. Therefore, as seen in the next section (1.2.2), glial cell, and in particular astrocytes, who display variations in intracellular calcium levels that correlate with neuronal activity and accomplish several important functions in brain can be observed and studied by imaging calcium. Making this tool, so far the only available technique to study brain network comprise of more than one cell type. The first calcium indicators developed were of synthetic nature, which are easily implementabel and have high signal-to-noise ratio [Stosiek et al., 2003], [Grienberger and Konnerth, 2012], [Wiederschain, 2011], [Helmchen and Waters, 2002], however they do not allow in principle to label genetically specified cell populations. To overcome this limitation came an important breakthrough from the

laboratory of the Nobel Prize winner Roger Tsien [Miyawaki et al., 1997]: the introduction of protein-based genetically encoded calcium indicators (GECIs). Combining these fluorescent calcium binding proteins with cell-type promoters, subcellular targeting sequences and transgenic technology, result in stable expression in specific cell subpopulations (Figure 5) over prolonged periods of time [Grienberger and Konnerth, 2012], [Knöpfel, Díez-García, and Akemann, 2006], [Looger and Griesbeck, 2012]–[Chen et al., 2013]. The applications of GECIs was initially restricted due to their small signal-to-noise ratios and slow response kinetics [Ohkura, Matsuzaki, et al., 2005,Tallini et al., 2006, Tian et al., 2009]. However, incredible progress in the development and refinement of brighter and more sensitive variants has been achieved during the last 15 years. Reaching, in some cases, performances comparable to those of synthetic calcium indicators [Horikawa et al., 2010, Palmer et al., 2011, Akerboom, Chen, et al., 2012]. Ultrasensitive genetically encoded calcium indicators of the GCaMP6-7 family [Chen et al., 2013] and RCaMP family [Akerboom, Carreras Caldéron, et al., 2013, Dana et al., 2016, Ohkura, Sasaki, et al., 2010] have been observed to be sufficiently sensitive as to report, under optimized experimental conditions, the calcium transients associated with the discharge of single AP in vivo.

1.1.4 2-photon calcium imaging

The design, development and optimization of fluorescent activity indicators opens the door to a wide range of possibilities and demonstrates that it is possible to monitor neural activity indirectly by capturing changes in the intracellular concentration of certain ions. But this is only half of the story, for the measurement and interrogation of neural or glial networks activity in the intact CNS with sufficient spatiotemporal resolution to actually take place it was necessary to produce fundamental advances in **optical imaging** [Grienberger and Konnerth, 2012, Bovetti, Moretti, and Fellin, 2014, Yang and Yuste, 2017]. The first approach used in combination with fluorescence indicators was standard wide-field fluorescence microscopy. This reprensents a minimal invasiveness approach with a large field of view and high spatial and temporal resolution, in the order of the μm and $ms - \mu s$ respectively. However, contrast and resolution strongly depend on labeling density, specially in highly scattering tissue, such as the mammalian brain [Denk and Svoboda, 1997]. Alternatively, confocal microscopy stands out as it overcomes some of the limitations of wide-field microscopy, improvement that is paid with signal loss (the pinhole rejects scattered photons coming from the focus), photobleaching and phototoxicity in out-of-focus planes [Pawley, 2006]. On top of that, in confocal microscopy excitation is achieved employing visible wavelengths, which are largely sensitive to scattering. These characteristics render standard wide-field and confocal fluorescence microscopy optimally suitable for studying thin samples, such as neurons in culture or superficial structures in biological tissue, but less appropiate for deep regions or large volumes of *in vivo* mammalian brain experiments.

To bring some light to this issue (pun intended) comes multiphoton micoscopy and in particular tow-photon laser-scanning microscopy (2PLSM). 2PLSM has seen its first

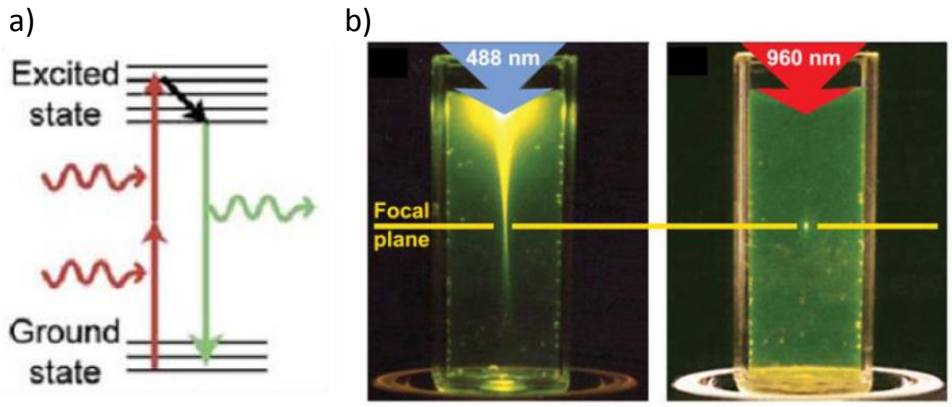

Figure 1.3: Two-photon excitation of fluorescent molecules. a) Simplified Jablonski diagram of the two photon emission process. Adapted from Svoboda and Yasuda, 2006. b) Experimental demonstration of the localization of excitation in 2P imaging using focused (0.16 NA) fs pulses of 960-nm light (right) in comparison to ingle-photon excitation of fluorescein by focused 488-nm light (0.16 NA) (left). Adapted from Zipfel, R. M. Williams, and Webb, 2003.

experimental validation around 20 years ago, and since then it has revolutionized biological imaging, due to its unprecedent high-resolution and high-contrast characteristics even when imaging hundreds of microns deep inside intact tissue [Denk, Delaney, et al., 1994], [Helmchen and Denk, 2005]. Briefly, 2PLSM is a laser-scanning method that exploits localized 'nonlinear' excitation to stimulate fluorophores only within a thin raster-scanned plane [Zipfel, R. M. Williams, and Webb, 2003]. Two-photon (2P) fluorophore excitation was first conceived by Marie Goeppert-Mayer [Göppert-Mayer, 1931] and relies on a simple yet very powerful concept which is the idea that when two photons arrive "quasi-simultaneously", that is within franctions of a fs, at the fluorophore, its energy is absorbed to promote the transition of one electron from the ground state to the excited state. The electron in the excited state then decays following the normal fluorescence-emission, or photochemical reaction, pathway as in single photon fluorescence excitation [figure 1.3a] [Pawley, 2006]. In this way, fluorophore excitation rely on higher-order light-matter interactions, thus having a non-linear dependency on the incident light intensity [Svoboda and Yasuda, 2006], [Helmchen and Denk, 2005]. This represents an improvement with respect to standard wide-field fluorescence, where excitation is due to absorption of a single photon and therefore depends linearly on light intensity. Three characteristics of 2P microscopy gives it a comparative advantage with respect to other approaches when imaging thick samples in vivo [Helmchen and Denk, 2005]:

1. **Imaging depth and phototoxicity**: 2P absorption in commonly used fluorophores

happens in the near-infrared wavelength range (700-1100nm). This frequency range is generally less phototoxic and penetrates deeper into scattering tissue than visible light.

2. **High resolution**: The fluorescence signal (S) depends on the square of the light intensity ($S \propto I^2$). Thus, when focusing the laser beam through a high NA objective, 2P absorption in non-saturating conditions is limited to the perifocal region [figure 1.3b] [Nagy, Wu, and Berland, 2005].

3. **No pixel cross-talk**: because the sample is sequentially excited, meaning that the signals are collected point-by-point, the pixel cross-talk observed in wide-field imaging is virtually absent.

Since the first validation of 2PLSM, progress has been made in several aspects: in the optical design of multiphoton microscopes, in probe engineering and in computational microscopy. This lead to higher signal-to-noise ratios, better temporal resolution, bigger field-of-view dimensions, penetration depth and accessible volume for in vivo imaging (reviewed in [Yang and Yuste, 2017]). It is currently becoming clearer and clearer that combining 2PLSM with fluorescent activity reporters constitutes one of the most powerful approaches to investigate the intact CNS at cellular resolution with cell specificity. In summary, 2PLSM allows the visualization of cellular activity in circuits of thousands of cells with single neuron resolution in the intact brain of behaving mammals. For these reasons the spatial navigation field has seen a recent increase in the implementation of 2P calcium imaging for the interrogation of hippocampal circuits [Gauthier and Tank, 2018, Rubin et al., 2015]. Together with appropiate analytical tools [Sheintuch et al., 2017], this approaches allow the study of discernable, trackable, cell specific ensambles of cells across days in awake behaving animals, opening the door the a whole range of questions that wold not be approachable otherwise.

However, as intense and productive all the before-mentioned (and much more that has not been mentioned here) research has been in the last decades, we can't help but to notice that it concerns only a subgroup of the full brain network: the neurons. But neurons represent approximately half of the cells in the brain, depending on the species can be more or less, the rest are **Glial cells**. Although glial cells don't have electrical activity like neurons have, they express rich calcium dynamics and interact with cells in active ways. In this work we will approach the question of if and what role play glial cells in spatial navigation in the mouse brain.

But first we will briefly describe the types of Glia cells that can be found in the brain, focusing specially on **Astrocytes**, the main actor of this work, their characteristics and the recent literature regarding its calcium signaling and its role in modulating neuronal activity.

1.2 Glia

Glial cells have been first observed as early as the mid 19^{th} century by Virchow [Virchow, 1856], and better described and brought to wider attention by Santiago Ramón y Cajal and Pío del Río Hortega a few decades later thanks to the development of chloride-sublimate technique, a staining technique that targets specifically astrocytes. At the time, glial cells were thought to play a strictly structural role in the brain. If anything else, the terminology used to describe them would be sufficient to understand the hypothesized role: described as *Zwishchenmass*, german for *inbetween mass*, *Nervenkitt*, or *nerve glue* in english, and finally the current terminology *Glial cell* comes from the Greek word *glía* meaning *glue*. It wasn't until the second half of the 20^{th} century when electrophysiological characterization and physiological studies of glial cells permitted the understanding of the wide range of vital functions that glial cells have in the functioning of the central nervous system [Morrison and de Vellis, 1981, Bowman and Kimelberg, 1984; Kettenmann, Backus and Schachner, 1984, Cornell-Bell et al., 1990a, Araque et al., 1998; Bezzi et al., 1998]. Phylogenic studies show that all organisms with a central nervous system have glial cells, and, interestingly, the ratio of astrocytes-to-neurons is different depending on the animal species and on the brain region, with intriguing correlates with brain complexity and neuronal density [Herculano-Houzel, 2011, Herculano-Houzel, 2014]. Throughout evolution, glial cells have diverge into specialized subgroups with different characteristics and function. The total glial population can be divided into four major groups: **microglia**, **astrocytes**, **oligodendrocytes** and their progenitors **NG2-glia**.

Unlike the rest of the glial cells, **Microglia** originate from yolk-sac progenitors that only populate the brain during development [reviewed in Kim and de Vellis, 2005; Kettenmann et al., 2011]. They represent the main immuno-competent and phagocytic cells of the central nervous system [Filiano AJ, Gadani SP, Kipnis J August 2015], and cover the major part of adult brain in individual non-overlapping domains. Microglia sense the environment through the movement of their filopodia, which rapidly reacts to abnormalities or damage [Nimmerjahn et al., 2005; Cronk and Kipnis, 2013]. Besides the inmuno-role, microglia has recently been hypothesized to have an active role in the healthy brain. Opinions on this matter are, however, controversial. While some studies show that microglia could be involved in motor-dependent synapse formation [Parkhurst et al. (2013)] and in features as high order as learning or social behavior [Torres et al., 2016, Kierdorf and Prinz, J Clin Invest. 2017], others have shown that ablation of microglia barely produce any alterations or pathologies in healthy adult mice [Elmore et al., 2014, 2015; Bruttger et al., 2015]. This discrepancies might be due to the major methodological differences in each study [Sarah Jäkel,and Leda Dimou 2017].

Oligodendrocytes are a type of large macroglia cells first observed by Pío del Río Hortega in the first half of the 20^{th} century. Their function is somewhat more clear: they insulate axons with self-produced myelin to allow a fast saltatory conduction and give

trophic support to axons [reviewed in Nave, 2010]. However oligodendrocytes have been found in sparsely myelinated brain regions, this presumably non-myelinating oligodendrocytes might have other functions that have been so far overlooked.

More interesting are the more recently discovered oligodendrocytes precursors, the **NG2-glia** cells [ffrench-Constant and Raff, 1986]. Their first more evident function is that of forming and maintaining a homeostatic network, preserving the cell numbers stable by generating mature myelinating oligodendrocytes throughout lifetime [Dimou et al., 2008; Rivers et al., 2008; Psachoulia et al., 2009; Simon et al., 2011, Hughes et al., 2013] under physiological conditions. What's really interesting about the NG2-glia cells is their ability to form functional synapses with neurons. A fenomena first observed in the hippocampus [Bergles et al., 2000] but later described in other brain regions [Karadottir et al., 2005; reviewed in Sun and Dietrich, 2013]. Such synapses are uniderectional in the sense that can only receive neuronal sygnals but can't generate action potentials on their own and further propagate them [De Biase et al., 2010].

The last large group of glia cells in the brain are the **Astrocytes**. Astrocytes and the effect of alterations on their calcium activity represent the main focus of this thesis. For this reason we will spend the next few sections on describing their function, anatomy and their known relation with neuronal activity.

1.2.1 Astrocytes

Astrocytes are the most abundant type of glial cell and represent up to 40% of all the cells in the mammalian brain [Herculano-Houzel, 2014]. Despite being one of the first glial cells to be discovered around 150 years ago, their description and the understanding of their role in the brain function is far from complete. As with everything in biology (is getting annoying really), astrocytes do not represent single homogeneous cell type and can be subdivided into several types depending on their morphology, molecular profile or function.

From the morphological point of view astrocytes can be roughly divided into two types: **fibrous** and **protoplasmic**. The first one is a star-shaped cell with regular contours present mainly in the white matter of the brain and spinal cord and in the optic nerve and the retina fiber layer. Fibrous astrocytes are characterized by their elongated morphology, with long processes running parallel to the axon bundles that make contact with myelinated axons and with oligodendrocytes. They have fewer processes compared to protoplasmic astrocytes. Their processes spatially overlap in their domains and extend to perivascular, subpial and axonal endfeet [Lundgaard et al., 2014].

Protoplasmic astrocytes on the other hand have a "bushy" and irregular morphology, with a small round somata of $\sim 10\mu m$ in diameter [figure 1.4]. Present $5-10 \sim 50\mu m$ primary processes, that further branch into thousands of branchlets and leaflets that form dense arborisations that connect with synapses [Bushong et al., 2002], and large endfeet that in turn connect with the vasculature [Nagelhus and Ottersen, 2013;

Verkhratsky, Nedergaard and Hertz, 2015]. Unlike fibrous astrocytes, protoplasmic astrocytes populate mainly the gray matter in the brain and have domains with well defined borders that do not overlap between each other [Bushong et al., 2002]. Even when the the area of influence of an astrocyte is limited to local domains and do not mix with other astrocytes, it is highly connected and has a strong influence in neuronal activity [schematically represented in figure 1.4]. A single astrocyte arborisation can cover 20,000 to 80,000 μm^3, contacting 300 to 600 dendrites and potentially 100,000 individual synapses [Bushong et al., 2002, Halassa et al., 2007]. This dense connectivity allows astrocytes to control several processes like ion homeostasis or neurontransmitter recycling. Interestingly, astrocytic domain boundaries have been proposed to be determined by, or at least closely relate to, neuronal functional units [Perea, Sur and Araque, 2014]. In this sense astrocytes could play the role of controlling and modulating *functional islands* formed by the synapses confined within the area of influence of a single astrocyte [figure 1.6c] [Halassa et al., 2007]. Further supports this hypothesis the fact that branching and connectivity of astrocyte, even from the same type, strongly depends on brain region. When comparing striatal and hippocampal astroglial populations it was noted that, despite having the same somatic volume, equivalent number of primary branches, and the same total cell volumes, hippocampal astrocyte territories are more constrained and display a tighter physical interaction with excitatory synapses [Chai et al., 2017] compare to striatal ones.

If astrocytes are so closely related to neuronal function and, as said before, have big and dense areas of influence, what are astrocytes functions in the brain? This question represents still a very active area of research. Here we will enumerate some of the known functions that astrocytes fulfill but will later describe in more detail the role of astrocytes in modulating neuronal activity.

Astrocytes are involved in the **control of cerebral blood flow** through **gliovascular coupling**. Matching the blood flow to the neuronal metabolic needs is crucial for healthy brain functioning, this is achieved by astrocytes in a two-fold manner. First by regulating dilation of blood vessels: it has been proved that synaptic activity mediates cytoplasmic calcium increases in astrocytes, that in turn promote dilation of neighbouring arterioles [Zonta et al., 2003, Attwell et al., 2010]. At the same time, astrocytes regulate vasoconstriction through the release of 20-hydroxyeicosatetraenoic acid (20-HETE) [Zonta et al., 2003, Metea and Newman, 2006]. Interestingly, astrocytes seem to *decide* weather to drive dilation or constriction based on local oxygen levels and metabolic states [Macvicar and Newman, 2015].

Given the enormous energy consumption in the brain, the regulation of oxygen and glucose availability must be tightly controlled. This is, of course, in part regulated by blood flow. However, while oxygen freely diffuses in the brain, glucose and other metabolites need specialised transporters to travel through cell membranes. The need for energy depends on neuronal activity, that can go from completely silent to high firing rate in miliseconds, which in turn can demand up to 30-fold increase in metabolic

consumption [Attwell and Laughlin, 2001]. It has been demonstrated that astrocytes, who are in contact both with blood vessels and synapses, strongly and tightly control active **metabolic support** to neurons. This can be achieved through a variety of processes that are still an intense area of study. Glucose is preferentially taken by astrocytes rather than neurons [Pellerin et al., 2007], that enters glycolysis and produces lactate. Lactate is then delivered to neurons via the astrocyte-neuron lactate shuttle (ANLS) [Pellerin and Magistretti, 1994)]. Meaning that astrocytes are not only involved in the metabolic support of neurons through blood flow regulation but also through direct delivery of energy substrates.

Astrocytes, together with microglia, have a key role in the **immune response** of the brain, both in physiological and pathological conditions. Upon brain injury or disease, astrocytes become reactive, drastically changing gene expression and entering full metal fight mode [Zamanian et al., 2012]. This changes induce morphological and functional alterations that lead astrocytes to enter one of two distinct reactivity profiles, depending on the nature of the insult. Inflammatory insult leads astrocytes to enter what has been called *A1*, a reactivity profile implied in synapse pruning suggesting a detrimental role. On the other hand, ischemic injury leads to activation of reactivity profile *A2* responsible for growth and survival of neurons and synapses, indicating a protective role. Such contrasting mechanisms coexisting in the same cell type proves once more, the complexity, diversity and specificity of astrocytic function. Moreover, in physiological conditions, astrocytes continue to play a role in immune protection of the brain by maintaining the blood-brain barrier (BBB). Interestingly, astrocytes have been shown to be involved in BBB formation during development [Hayashi et al., 1997].

Besides the aforementioned functions, astrocytes play key roles in Ion [Sibille, Pannasch and Rouach, 2014, Nwaobi et al., 2016], water [Nielsen et al., 1997, Risher, Andrew and Kirov, 2009] and neurotransmitter [Danbolt, 2001, Herman and Jahr, 2007] homeostasis. Astrocytes can rapidly change their volume and intercellular communicative capacity, which allows them to redistribute water across astrocytic networks. Can redistribute K^+ ions through K^+ spatial buffering, and are the only cells in the central nervouse system that can synthesize glutamate and GABA from glucose. Astrocytes are an incredible versatile and complex cell that account for an incommensurate amount of functions and roles in the brain, however the aspect of astrocytes that concerns this work relates to the signaling in astrocytes and its relation with neuronal activity. We will discuss this aspects next.

1.2.2 Calcium signaling in astrocytes

As inexpert scientists, we PhD students have a bias view of the way research works towards positive discoveries and confirmed hypothesis. Simply because our biggest source of information are publications, and the chances of getting a story published that states "we formulated **this** hypothesis, and found it to be wrong" are very low, there's a lack of charm in failure that prevents unsuccessful hypothesis to be known.

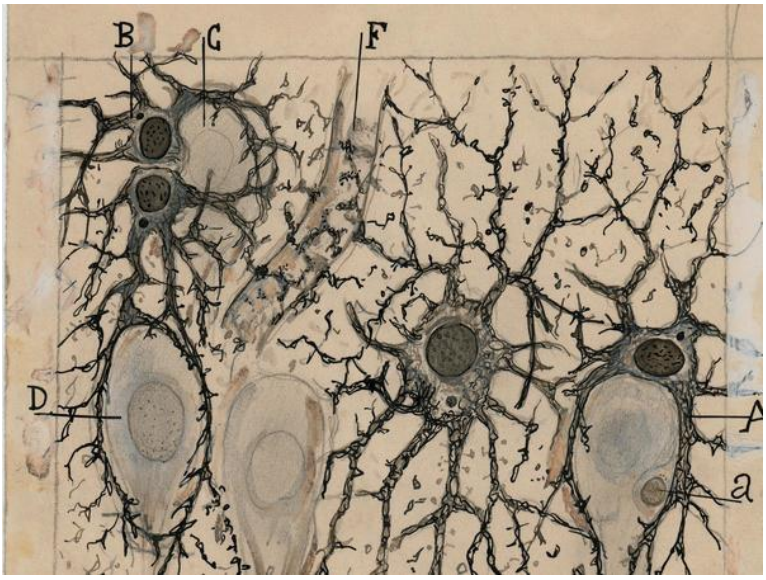

Figure 1.4: One of Cajal's original drawing of astrocytes in the hippocampus of a man three hours after death. This beautiful representation exemplifies several of the properties of astrocytes discussed here. Note the connections with blood vessels, the small overlapping area of domains, the somas, large and distal processes and how astrocytic processes surround neuronal cell bodies.

Which is regrettable, because proven wrong hypothesis are at least as informative as positive results. With brilliant examples like the Michelson-Morley experiment in 1887, where the two physicist trying to prove the existence of the aether, the medium in which light was thought to propagate, proved instead that it didn't exist. And in the way invented the interferometer. Invention that was later crucial for the development of the special theory of relativity and, more recently, for the detection of gravitational waves. We can go even further and say that logic allow us *only* to falsify theories, but, on the other hand, to prove a theory *correct* is impossible. We can get encouraging results, experiments that help us gain confidence in our working hypothesis, but not really prove it. On the other hand, one counterexample is all that is needed to prove it wrong. As Einstein eloquently put it:

> *The scientific theorist is not to be envied. For Nature, or more precisely experiment, is an inexorable and not very friendly judge of his work. It never says "Yes" to a theory. In the most favorable cases it says "Maybe", and in the great majority of cases simply "No". If an experiment agrees with a theory it means for the latter "Maybe", and if it does not agree it means "No". Probably every theory will someday experience its "No" —most theories, soon after conception.* [Albert Einstein: the human side: New glimpses from his archives. Dukas and Hoffman 1922]

Perhaps a way to compensate for this bias is to get rid of the miss-conception that falsifying an hypothesis represent failure but instead call it for what it is, a scientific discovery.

In a way, a fruitful, but less interesting substitute of self-falsified hypothesis are the stories of scientist trying to prove *other* peoples theories wrong, because controversy, unlike failure, sells journals. One of the highly interesting and still active controversies in neuroscience is the question whether calcium concentration elevations in astrocytes regulates neuronal and vascular function. This has led in the last few decades to a series of works by different groups that appeared to be contradictory, and different research lines have been seemingly proving each other wrong to give rise to a better and more profound understanding of the subject. We will not refer here the complete story that has been brilliantly summarized by Bazargani and Attwell [Bazargani and Attwell 2016], but will refer only some characteristics of calcium signaling in astrocytes that are relevant for the understanding of this work.

It's important to note first, that astrocytes, unlike neurons, are non-excitable cells. For this reason, Ca^{2+} fluctuations have been considered as the main intracellular readout of detection of environmental changes. That includes astrocyte-neuron communication. An extensive amount of work in the last few decades has been dedicated to understand the origin of Ca^{2+} transients, if this fluctuations are somehow relevant for neuronal regulation, and if so, how. To the date most of this questions remain unanswered, although currently there seems to be a common consensus in the field that (spoiler alert) they are at least involved in several regulation pathways, and respond, in physiological conditions to behavioral and sensory correlates.

Should caught our attention the fact that baseline levels of Ca^{2+} in astrocytes are higher than that of neurons, and that this concentration vary inside each cell, being higher in processes compared to the soma [Zheng et al., 2015]. Which already suggest two observations: first, the relevance of Ca^{2+} in astrocytic signaling, and second, the within-cell complexity of it [figure 1.5]. In astrocytes, Ca^{2+} fluctuations can have different sources, the first of which is intrinsic. In fact, it was shown that 65% of astrocytes in hippocampal slices exhibit asynchronous and localised Ca^{2+} transients, even in the absence of neuronal activity [Nett et al., 2002]. The role and relevance of these untriggered events has yet to be defined. Specially because it's unclear if this spontaneous events do happen in physiological conditions and if so, in which fashion.

More interesting are Ca^{2+} **changes induced by neuronal activity**. Glutamate has been shown to evoke calcium concentration rise in astrocytes in several contexts, in culture [Cornell-Bell et al., 1990], in brain slices [J.W. Dani et al., 1992], in whole retina [Newman and Zahs 1997] and *in vivo* [Wang et al. 2006]. This calcium transients can propagate along astrocyte processes and even between glial cells [ornell-Bell et al., 1990, J.W. Dani et al., 1992, Hirase, H. et al., 2004, Nimmerjahn, A. et al., 2004]. This observations further support the possibility that glial Ca2+ waves might constitute an extra-neuronal signaling system in the CNS, and, importantly, that it can be driven by neuronal activity. However, to begin to understand the neuron-astrocytic Ca^{2+} activity relation one must realize that, just like neurons, astrocytes have to be thought as

the sum of many different subcellular compartments and that calcium transients occurring in the soma are very different [figure 1.5] and can have different sources as the the ones in fine astrocytic processes near synapses. Ca^{2+} events in processes can occur independently of larger ones in the soma, which suggest that regulation of synapses or blood vessels can happen locally. This events can, however, propagate to neighbouring intracellular areas [Di Castro et al., 2011] or even synchronise with neighbouring cells [Takata et al., 2013]. Importantly, it has been shown that such events correlate with the strength of neuronal activity [Panatier et al., 2011].

Process and soma Ca^{2+} events also differ in their temporal profile. While is true that somatic calcium transients are several order of magnitude longer than neuronal action potentials, which has been an historical argument against the hypothesis that astrocyte could be involved in real-time information processing in the brain, smaller events occur in processes even in the subsecond scale [Winship, Plaa and Murphy, 2007; Lind et al., 2013, 2018]. This partially solves the temporal argument, but in a more fundamental aspect, it's by no means clear if information processing in neuronal network relies in temporal or rate coding or a combination of both. Rate coding responses could be an alternative way in which long lasting astrocytic Ca^{2+} signals could be involved in a relevant temporal scale in neuronal activity and information processing [Semyanov, 2019]. On a further bigger scale, Ca^{2+} events can propagate as waves through networks of several tens and even hundreds of astrocytes. Behavior that has been observed in cultures [Cornell-Bell et al., 1990b], as well as *in vivo* in the frontal and parietal cortices upon sensory stimulation []Ding et al., 2013] and in the cerebellum during locomotion [Nimmerjahn, Mukamel and Schnitzer, 2009]. Giving rise to the possibility of astrocytes modulating neuronal activity at a network scale. As stated before, many of such calcium transients have been shown to depend, or have its origin in neuronal activity dependent processes. In hippocampal dentate gyrus astrocytes action potential–driven synaptic transmitter release triggers large and long lasting ($\sim 3s$), spatially broad ($\sim 12\mu m$) events, while spontaneous synaptic transmitter release produces brief ($\sim 0.7s$), spatially localized ($\sim 4\mu m$) transients [Di Castro, M.A. 2011]. It has been suggested that release of Ca^{2+} from internal stores could be the main source of Ca^{2+} somatic transients, while in the astrocyte processes transmembrane entry of Ca^{2+}, presumably through endogenously active channels such as TRPA1 [Shigetomi, 2012] or receptor-gated Ca^{2+}-permeable ion channels, generates 30–40% of Ca^{2+} concentration elevations. In this way while Ca^{2+} rises in astrocyte somata may be too slow [Schummers, et al. 2008, Schulz, K. et al, 2012] to generate rapid blood flow increases, Ca^{2+} transients in the processes that are faster than in the soma [Tang, W. et al. 2015] occur before or with a similar time course to the increase of blood flow [Lind, B.L. 2013, Otsu, Y. et al, 2015].

We will not dig into the specific mechanisms through which neuronal activity could induce such calcium transients (related to the activation of mGluR receptors by glutamate release) or the controversies involved. But will instead mention some of the observations that evidence astroctytic calcium transients physiological relevance. It

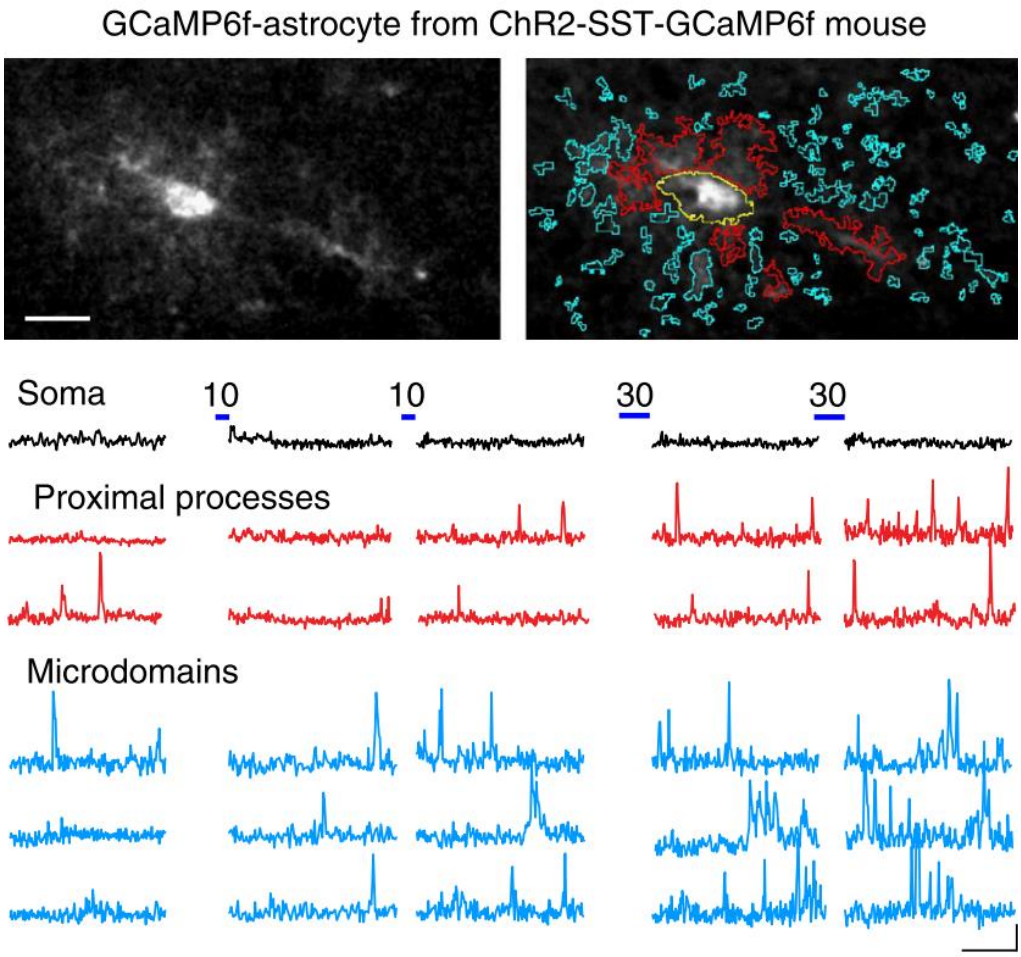

Figure 1.5: Astrocytes present complex calcium transients in their somas and processes. Image of GCaMP6f-astrocyte in layer 2/3 SSCx from an adult ChR2-SST-GCaMP6f mouse that undergo SST interneuron optogenetic stimulation. ROIs are depicted for the soma (yellow), proximal processes (red) and microdomains (blue), scale bar is 20 μm (top). Calcium signal dynamics at example compartments show the difference between transients depending on the region of the astrocyte, scale bars is 50s, 20%$\frac{dF}{F0}$. Adapted from Mariotti et al., 2018.

has been observed that whisker stimulation increases Ca^{2+} concentration in astrocytic cytoplasm in the barrel cortex [Wang et al., 2006], in a frequency dependent manner [Perea and Araque, 2005; Sherwood et al., 2017]. Other behavioural variables like locomotion or arousal state have been observed to evoke Ca^{2+} elevation over broad spatial areas, mediated by noradrenaline signals in the frontal and parietal cortex [Ding et al., 2013, Paukert, et al., 2014]. Suggesting an astrocytic involvement in the control and modulation of sensory input and behavior.

1.2.3 Astrocityc modulation of neuronal activity

The complexity both in source and dynamical properties of calcium oscillations in astrocytes makes it rather complicated but at the same time extremely interesting to study. We've seen that astrocyte calcium changes are related to neuronal activity, to neurotransmitter release and to sensory input and behavioral state. That they can occur in fast transients in the processes or in longer, stronger events in the soma. That can propagate within the cell, across neighbouring cells and through extended networks. This covers one way of information flow in the *extended brain network* (that is considering neurons and glial cells). But what is the role (or roles), if any, of each of this astrocytic calcium dynamics in the processing of information by neuronal networks? In other words, how does astrocytic activity modulate neuronal functioning? We are interested in the answers to this questions that are related to the brain information processing and its meaning for behavioural outputs, and therefore to the astrocytic-induced changes in neuronal properties.

Given that astrocytes extend processes that are ideally positioned for dynamic exchange with the synapses [figure 1.6a], the first observations are related to how astrocytes influences synapses. This happens in three aspects: by regulating **presynaptic release probability**, **postsynaptic receptor activation** and **synaptic plasticity**. Importantly, release of gliotransmitters, which is one of the key ways in which astrocytes comunicate with neurons, is widely accepted to follow cytoplasmic Ca^{2+} rise in astrocytes, making Ca^{2+} transients highly relevant for the comunication between neurons and astrocytes and its experimental testing. However, we have to keep in mind that gliotransmitters can have different effects depending on the target, the neuronal activity regime, the brain region, and the developmental state to be able to properly interpret the extended network activity.

At the **presynaptic level**, it has been observed that in the dentate gyrus, astroglial glutamate release activates presynaptic NMDA receptors, potentiating excitatory transmission [Jourdain et al., 2007]. Similarly, in the hippocampus proper glutamate potentiate transmitter release, although in this case by activating presynaptic mGluRs but without the intervention of NMDA receptos [Perea and Araque, 2007; Navarrete and Araque, 2010]. Astrocyte release of glutamate has been observed to mediate not only excitation but also inhibition at the presynaptic level during sustained neuronal activity. This is achieved in two ways, first by binding presynaptic kainate receptors that

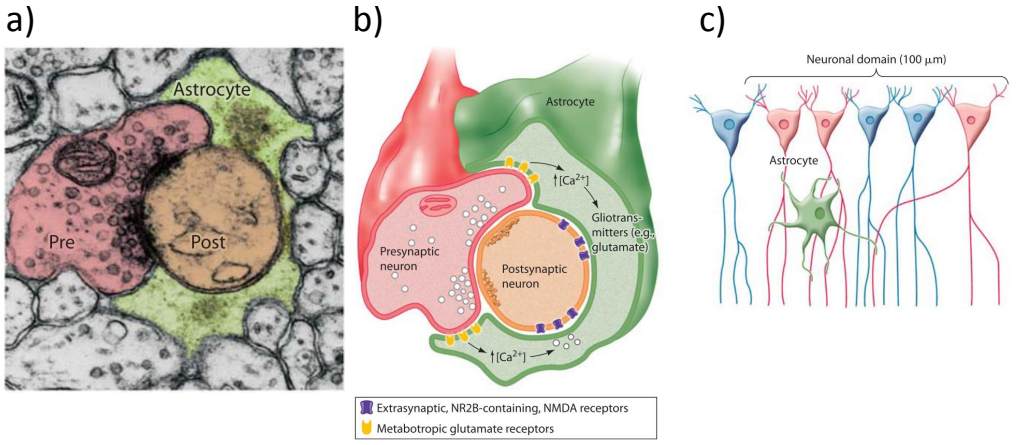

Figure 1.6: Astrocytes form tripartite synapses with pre- and postsynaptic neurons that modulate neuronal activity at several levels. a) Electron microscopy shows the tripartite nature of synaptic structures with astrocytic processes (green) associating with pre- and postsynaptic terminals. Adapted from Mariotti et al., 2018. b) Schematic representation of a) where, in the hippocampus, metabotropic receptors in the plasma membrane of the nearby astrocytic processes is activated by glutamate released from the presynaptic Schaffer collateral terminals. As a result of this activation intracellular Ca^{2+} increases in the astrocytes, which in turn lead to the release of glutamate from glial cells through the fusion of tetanus toxin-sensitive vesicles. Astrocytic glutamate selectively acts on extrasynaptic, NR2B-containing NMDA receptors to trigger slow inward currents (SICs) in pyramidal CA1 neurons. c) Schematic representation of the mechanisms by which a single astrocyte (green cell) through glutamate release can lead to neuronal synchronization of local clusters of neurons or neuronal domains (red cells). b) and c) adapted from Fellin, Pascual, and Haydon, 2006

strengthen inhibitory synaptic transmission [Kang et al., 1998; Liu et al., 2004], and second, Ca^{2+} uncaging-mediated glutamate release from astrocytes produce binding of presynaptic mGluRs in neurons that in turn decrease evoked postsynaptic currents in the hippocampus [Araque et al., 1998]. It has been recently shown that single astrocyte may release different gliotransmitters [Covelo and Araque, 2018], which can induce more complex modulation of synapses: high frequency stimulation of the CA3-CA1 projection in the hippocampus produced finely tuned release of both glutamate and adenosine from astrocytes, modulating synapses in a biphasic way. Initial glutamate release induced potentiation followed by purinergic-mediated depression of neurotransmitter release, which represents an elegant example of the subtle and complex modulation effects of neuronal comunication by astrocytes [figure 1.6b].

At the **postsynaptic level** it has been observed that disrupting gliotransmission in a dnSNARE mouse model produced a hypofunction of postsynaptic NMDA receptors, which has effects at the network level affecting cortical slow oscilations (see bellow) [Fellin et al., 2009]. Similarly NMDA receptors binding have been shown to be modulated by astroglial D-serine release, which in turn modulates glutamatergic synaptic transmission [Panatier et al., 2006, Henneberger et al., 2010]. Astrocyte gliotransmission has been observed to have effects in **synaptic plasticity** and memory. Clamping

Ca^{2+} in individual CA1 astrocytes blocks LTP inductions at nearby excitatory synapses by decreasing the occupancy of the NMDAR co-agonist sites [Henneberger et al., 2010]. Exogenous D-serine or glycine application reverse this effect. Note that this Ca^{2+}-dependent release of D-serine from an astrocyte control of NMDAR-dependent plasticity can potentially affect many thousands of excitatory synapses but only those that are nearby, implying a local regulation of neuronal activity. This further advocates for the functional spatially localized aspect of astrocytic domains. Conversely, astrocytes can also modulate synaptic depression. Ca^{2+} clamping in rat barrel cortex astrocytes during development showed impaired t-LTD [Min and Nevian, 2012]. Moreover, simultaneously stimulating an astrocyte with depolarising pulses and afferent fibres resulted in LTD. This result suggests that astrocyte signalling is sufficient to induce plasticity at the level of neuronal synapses. Finally, astrocytes have been shown to be involved in the synaptic depression of untetanised synapses paralleling LTP in the hippocampus [Pascual et al., 2005; Serrano et al., 2006; Andersson, Blomstrand and Hanse, 2007; Chen et al., 2013]

There are several mechanisms through which astrocytes modulate **neuronal excitability**, that is, neuronal electrical dynamics during action potential firing. Action potentials or spikes in neurons depend on the fine and complex relation between ionic concentrations withing neurons and in the extracellular space, which is in turn regualted by the activity of voltage-gated ion channels. One of the most consolidated functions of astrocytes is the maintenance of ionic homeostasis and more specifically the buffering of extracellular potassium [Kofuji and Newman, 2004, 2010; Kimelberg and Nedergaard, 2010; Hertz and Chen, 2016]. The rapid intake of K^+ by astrocytes prevents neuronal hyperexcitability [Bellot-Saez et al., 2017]. Although the specific intracellular mechanisms are not clear, there has been strong evidence towards the idea that astrocytes, through the secretation of purines set neuronal firing thresholds, both in pyramidal cells and interneurons [Kawamura, Ruskin and Masino, 2010, Kawamura et al., 2004, Tan et al., 2017].

We mentioned how astrocytes modulate each side of the synapse and synaptic plasticity and later how they influence neuronal excitability. Continuing with the growing scale progression, astrocytes play key roles in the **synchronization of neurons** and at the **network level**. As we stated at the beginning of this section, the mechanisms through which astrocytes influence neuronal activity depend on cell type, brain region and developmental state of the animal. In the absense of neuronal activity hippocampal CA1 neurons present inward currents with slow kinetics found to be mediated by glutamate released from astrocytes, simillar to those observed under stimulation of Schaffer collaterals [Fellin et al., 2004]. This response occurs synchronously in multiple CA1 neurons, evidencing the functional role of astrocytes in the synchronization of neurons [figure 1.6c]. More recently, it has been observed that cellular coordination might not involve inter-astroglial Ca2+ spread, suggesting other mechanisms of astroglial networks cell coordination [Chever et al., 2016]. However, neuronal network oscilations

or brain waves are not restricted to the hyppocampus, instead they are present in almost every brain region, during sleep, sensory perception, can have functions that vary from memory consolidation to temporal coding (as mentioned before) and lie in a wide variety of frequency and power bands. The mechanisms by which network oscillations are formed and modulated are still a matter of intense study. Interestingly, it has been recently proposed that astrocytes might play a role in the regulation of neuronal membrane potential oscillations at a wide range of frequencies [Bellot-Saez et al., 2018]. Indeed blockade of K^+ uptake or astrocytic connectivity, enhance network excitability and form high power network oscillations. This could be due to changes in the oscillatory behaviour of individual neurons, which is a well known effect in the system dynamics field. More precisely it has been shown that, as we mentioned before, impairing gliotransmission altered slow wave dynamics in the cortex by reducing neuronal depolarization periods duration, and prolonging hyperpolarization [Fellin et al., 2009]. Moreover, slow oscillations involves oscilation in neuronal membrane potential as well as astrocytic calcium dynamics, with the latter preceding neuronal changes. And alterations in astrocytic calcium dynamics inhibits slow wave activity, showing the fine causal interplay between both types of cells during brain oscillations [Szabó et al., 2017]. Finally, astrocytic signaling has been observed to be involved not only in gamma oscillations but also in their cognitive correlates [Lee et al., 2014], being this an example of how astrocytes acitivity is crucial for proper performance in tasks as high order as novel objet recognition.

We couln't and wouln't try to make a full description of the vast plethora of mechanisms by which neurons and astrocytes interact, or the function of each of this interactions, many of which are a matter of active debate to date. Heterogeneity in experimental procedures might account for some of the discrepancies in the literature. But we hope we've built so far the case that astrocytes, and in particular astrocytic Ca^{2+} dynamics, is involved and regulates the way the brain process information. It does so at the level of the synapses, in single cells, and at the network scale. That this interactions go both ways, with astrocytes modulating neuronal dynamics but also neuronal activity interfering in astrocytic profiles. That the complexity and richness of this modulation extends not only to the spatial domain but also at the temporal scale, with small fast and local interactions as well as large waves of activity spanning whole brain regions. And more important, that when studying the way the brain solves a task, considering only neuronal networks might not be enough, and a shift in the paradigm towards the study of an extended neuronal-glial networks might be needed.

1.2.4 Astrocytes accumulate evidence

So far we've discuss how astrocytes are involved in the way in which neurons process information, focusing mainly in the mechanisms by which such interactions might take place. However, to further develop the idea of the brain acting as an extended network of both neurons and glial cells during the processing of information, we are inclined

to ask the complementary question whether astrocytes or astrocytic networks process information themselves, and if so, how.

The pursuit of the answer to this question has produced very recent findings that bring some light to the matter, as well as pose more questions. Misha Ahrens group studied the interplay off astrocytic and neuronal networks during swimming adaptation strategies and information integration in larval zebra fish [Yu Mu, et al., 2019]. In this task animals were exposed to a virtual reality environment where visual feedback was eventually decoupled from motor actions so that the swim behaviour would fail to trigger the expected visual flow. The animals, after becoming aware of the futility of their efforts would became passive and stop motion, to then try again a few seconds later [figure 1.7a]. When animals switched from the active to the passive behavioral state, whole-brain average neuronal activity decreased while glial activity increased. In this case, activity refers to Ca^{2+} transients that started seconds before and peak after passivity onset [figure 1.7b].

The availability of chemical, optical and genetic tools allows interventional approaches that can test this hypothesis from a causal point of view. Reduction of astrocytic Ca^{2+} activity by two-photon laser ablation of glial cells or blocking the inositol 1,4,5-trisphosphate receptor to reduce Ca2+ release from intracellular stores, led to a reduction in futility-induced passivity. Using a chemogenetic approach to increase intracellular Ca^{2+} in glia on the other hand led to an increase in the time spent in passive state. This effect was temporally tuned as shown by optogenetic activation (either using CoChR or Opto-a1-AR). Which suggests that astrocytic Ca^{2+} are necessary and sufficient for the expression of this behavior.

Interestingly, the way astrocytes exert this effect on behavior is achieved through a finely tuned interplay between neuronal and astrocytic networks. More precisely during futility-induced passivity, signals from noradrenergic (NE) neurons together with local circuit activity triggered glia responses as proved by optogenetically activating NE neurons. Showing that astrocytes integrate both behavioral information as well as NE signals. Astroyctes, in turn, activated GABAergic neurons that would most likely supress swimming.

The question that interests us the most is what is the *information* processing that is done in each step of this complex behavior by each element of the network? Through a series of complex but very elegant probabilistic experiments, the group demonstrated that NE neurons signals encode sensory-motor mismatch signal. Signals that are transmitted to astrocytes that in turn *accumulate evidence* that actions are futile and control, through GABAercig neurons, swimming behavior [figure 1.7c].

This example beautifully puts together several of the functions and characteristics of astrocytes discussed previously in a orchestrated mechanisms with a behavioural output with high level of complexity. It shows in a physiological and behavioural relevant way, how astrocytes are involved in network state changes, how they integrate neuronal activity, modulate downstream circuits, influence behavior and importantly,

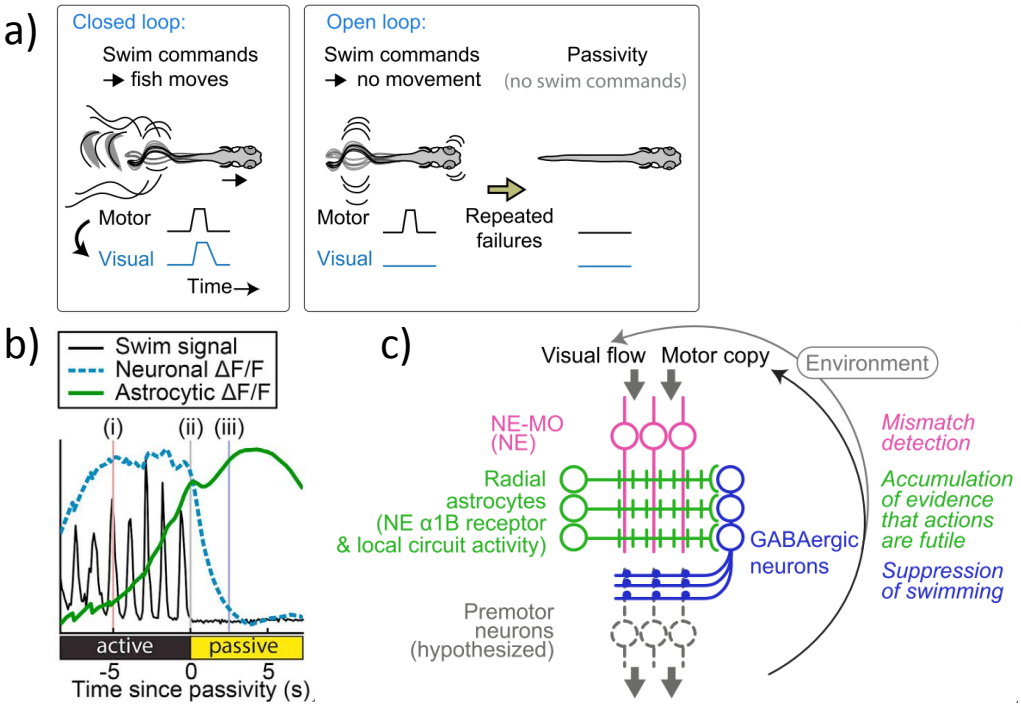

Figure 1.7: Astrocytes in the zebrafish accumulate evidence. a) Locomotion in closed loop versus open loop. zebrafish entered a passive behavioral state after repeated swim failures. b) Averaged neuronal and glial signals near passivity onset for one representative animal. Average neuronal calcium activity decayed after passivity onset, while glial calcium activity increased before passivity onset and peaked soon after. c) Schematic representation of the circuit hypothesized by the authors: mismatch signal computed from visual and motor efferent inputs are represented by specific neuronal circuits. These neurons noradrenergic axons excite glial processes belonging to astrocytes that integrate mismatch signals and supress swimming through the activity of downstream GABAergic neurons. Adapted from Mu et al., 2019.

process information in complex and functional ways. It evidences how to uncover the underlying functional role of astrocytes it is sometimes necessary to see the big picture and perform experiments and tasks closer to ethological behaviours.

Only days ago, another elegant example of how astroyctes are involved in complex behavior modulation has been published [Seungwoo Kang, 2020]. The group showed that in mice, astrocytes from the dorsomedial striatum differentially regulate medium spiny neurons activity facilitating shifts from habitual to goal-directed reward-seeking behavior. And they do so by tuning excitatory and indirect inhibitory postsynaptic currents in neurons, process regulated by adenosine metabolism, receptor signaling, and transport. This examples manifest, however, the complexities of the experimental procedures needed for proper understanding of network functioning during complex behaviors *in vivo*.

1.3 Astrocytes encode spatial information in Ca^{2+} activity

Finally we'll summarize recent unpublished work from our lab, that settled the basis for the work in this thesis. As we've seen, astroyctes are involved in the processing of information in the brain, both by encoding specific aspects of behavioural variables and the relation with the environment and by interacting with neuronal networks. Astrocytes and their interactions with neurons have been extensively studied in the hippocampus [Perea and Araque, 2007, Pascual et al., 2005; Serrano et al., 2006; Andersson, Blomstrand and Hanse, 2007; Chen et al., 2013, Covelo and Araque, 2018], however as discussed in the first part of this introduction, one of the most interesting and thoroghly studied functions of hippocampal networks is the encoding of spatial information and the building of a cognitive map for spatial navigation. The question whether hippocampal astroctyes intervene, alter or modulate spatial information encoding in neurons or, more fundamentally, if navigational information is encoded exclusively in neuronal cells or it involves the extended brain network comprising glial cells as well as neurons had not been elucidated to date. Our lab has tackled this question by specifically asking how astrocytic calcium signaling relates to spatial navigation, with the working hypothesis that astrocytes encode navigational information in their intracellular calcium dynamics.

There are, however, a few remarks that are needed to understand the following results and the research exposed in this thesis. So far we have been talking about *information*, *information flow* or *encoding of information* in a rather loose way, without defining what we really mean. However, throughout this work, **information** will have a very well defined and concrete meaning, and that is the one established by **information theory**. We'll explain these concepts in the next section.

1.3.1 Information Theory

Information theory was first developed by C. E. Shannon and beautifully exposed in his landmark paper *A Mathematical Theory of Communication* [Shannon, 1948]. In it, Shannon develops a mathematical formalism of communications, considering the coding an decoding problem of information in noisy channels. This theory has extended to many fields with several practical and theoretical applications, notably modern computation, quantum mechanics, quantum computation and neuroscience. There are several ways of approaching the notion of information as in Shannons theory, we will expose a modified version of the one exposed in his paper. We'll take his approach first because it relates information to probability distributions in an intuitive way which is what we need, second because of its comprehensibility and third because, in a slightly more abstract sense, the brain can be thought as a noisy communication network, with neurons being both transmitters and receivers. However, it's useful to keep in mind what's the objective, what is it that we are trying to use information theory for. The question we'll try to answer is: if we look at neuronal activity, how much information do we gain from a certain behavioral variable (for example the position of the animal)?

Lets try to formalize the problem: neurons can be in several states, depending on how we describe them. We can think of a neuron as a variable with two states, either firing or not, or with a continuum of states, like all the possible values of its membrane potential or of the calcium concentration inside the cell. Lets consider then in a general way that each state of the neuron has a certain probability, namely state x has probability p_x of occurring. When we observe a neuron we gain information about its state, the neuron was either firing or not. However before measuring it we can ask the question of **how uncertain are we about the state of the neuron if we know the set of probabilities** $\{p(x)\}$. This is equivalent to asking the question of *how much* information we gain when we learn the state of the neuron. In this example we are using the state of a neuron, but the approach is general to any probability distribution. To answer a 'how much' question (either uncertainty we have or information we gain) we need a quantitative measure, lets call this measure H. There are three rather reasonable properties that we'd like to ask of H:

- H **should be a function only of the probabilities**, it doesn't matter if it's neuron 1, 2 or Z, if it's a principal neurons or an interneuron (or an astrocyte) as long as the probabilities of its states are the same, therefore we can write $H(p_x)$. And H **should be continuous in** p_x.
- If all the events are equally possible, that is $p_i = \frac{1}{n}$ with n the amount of states, then H **should be a monotonic increasing function of** n. Intuitively, if there are more possible states, and all the states are equally possible, there is more uncertainty.
- The information gained when two independent events occur with individual probabilities p and q is the sum of the information gained from each event alone.

It can be proved that the only H that satisfies all three properties is of the form:

$$H = -K \sum_{x=1}^{n} p_x \, log(p_x) \tag{1.1}$$

with K a positive constant that amounts only to the choice of units of measure. This expression might ring a bell for those who have studied statistical mechanics, H is nothing but the **entropy**. We select the logarithm to be in base 2 (all logarithms in this thesis will be in base 2 unless otherwise specified), which is achieve by appropriately selecting the constant K, and define the entropy of the probability distribution $p_1, p_2, ..., p_n$ of an n state variable as:

$$H = -\sum_{x=1}^{n} p_x \, log_2(p_x) \tag{1.2}$$

This definition is intuitive but is not the whole story. Probably the best reason to define entropy in this way is because it can be used to *quantify the resources needed to store information*. It can be proved that Shannon's entropy represents the minimal physical resources required to store the information being produced by a source, in such a way that at a later time the information can be reconstructed. This result is known as the *Shannon's noiseless coding theorem* [Shannon, 1948].

It might be useful to build a toy example to illustrate some of the properties of H. Lets consider an overly simplified neuron with two possible states, it can be either firing or not. It fires with probability p and is silent with probability $q = 1 - p$, then its entropy is given by

$$H = -(p \, log(p) + (1 - p) \, log(1 - p)) \tag{1.3}$$

We can see the values of H as function of p in the figure 1.8a. If the neuron would always be silent and never fire, we'd have no uncertainty of its state and we would gain no information by measuring its state. In this example that is represented by $p = 0$ and therefore $H = 0$. If, on the other hand, the neuron would fire randomly half of the time, we would have absolute uncertainty about its state before measuring and therefore we'll gain the maximum amount of information after measurement. That is, its probability of firing would be $p = 0.5$ and the entropy would be $H = 1$. Meaning that knowing the state of the neuron gives us 1 bit of information. In general we have that $H = 0$ if and only if all $p_i = 0$ except one that is 1, and the uniform distribution is the probability distribution with maximum entropy and the entropy is the logarithm of the number of states. That is $H = log(n)$ and is maximum if and only if $p_i = \frac{1}{n} \; \forall \; i$.

Now, before we tackle the question that brought us to this point to begin with, we have to define other important quantities from the theory. Let's say we have another variable with its own states and probability distribution $p(y)$, that can represent another neuron, or set of neurons, or a behavioral variable like the position of the animal. We define the **joint entropy** of variables X and Y as

$$H(X, Y) \equiv -\sum_{x,y} p(x, y) \, log(p(x, y)) \tag{1.4}$$

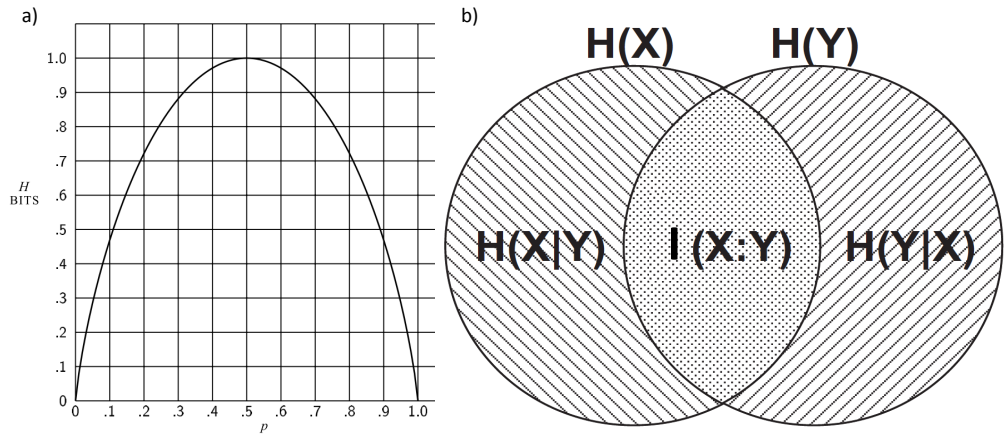

Figure 1.8: Concepts of entropy and information theory. a) Entropy of a binary variable as a function of the probability p, adapted from Shannon, 1948 b) Schematic entropy and information Venn diagram, adpated from Nielsen and Chuang book, 2010.

The joint entropy measures our total uncertainty about the pair (X, Y). Now, suppose we learn the value of Y, meaning that we gained $H(Y)$ bits of information about the pair (X, Y). How much uncertainty remains about the pair (X, Y)? Or in other words, how uncertain are we about X, given that we know the value of Y? This quantity is called the *entropy of X conditional on knowing Y* and is defined as

$$H(X \mid Y) \equiv H(X, Y) - H(Y) \tag{1.5}$$

Now we have everything we need to define the quantity that would answer our initial question that was: if we look at neuronal activity, how much information do we gain from a certain behavioral variable (for example the position of the animal)? We can reformulate this question into an analogous form and ask, how much information is shared between neuronal activity and the behavioral variable? In a general way, lets consider two variables X and Y, suppose we add the information content of X, $H(X)$ to the one of Y, $H(Y)$. If there's information shared in the two variables, then we will be counting it twice, and information that is not common will be counted only once. So if we subtract then the total amount of information of the pair, which is nothing but the joint entropy $H(X, Y)$ what will remain is the common or the **mutual information** of X and Y:

$$I(X : Y) \equiv H(X) + H(Y) - H(X, Y) \tag{1.6}$$

In the last paragraph we have been using *information* and entropy as interchangeable concepts. That is because, as we said at the beginning of this section, entropy quantifies the amount of uncertainty about a variable before knowing its state or equivalently, how much *information* we gain when we measure its state. However, we could arrive

to the expression for mutual information in a slightly different but equivalent way that might be more reassuring about the use of the term *information*. Recall that *conditional entropy* $H(X \mid Y)$ represents the uncertainty that remains in X given that we learned the value of Y. Thus, the complement of the uncertainty that remains is the *information we gained* about X by knowing Y. Formally, we can define *mutual information* then as

$$I(X:Y) \equiv H(X) - H(X \mid Y) \tag{1.7}$$

The equivalency of this two expressions 1.6 and 1.7 is trivially shown simply by replacing 1.5 in 1.6. The various definitions and relationships between entropies might be difficult to picture or remember. A useful way of visualizing them is using the 'entropy Venn diagram' shown in figure 1.8b, which is not completely reliable as a guide of the properties of entropy but can provide a comprehensible mnemonic.

Information theory has been widely used and studied in neuroscience. With works as early as Richmond and Optican in the 1990 [Richmond and Optican, 1990] on the primate visual cortex or Skaggs formula for spiking activity in 1993 [Skaggs et al., 1990]. There are several reasons for the success and usefulness of information theory approaches for studying the brain. First, information theory is model independent, in the sense that we are not required to explicitly specify what is our model of the interaction between the variables of our system. This does not mean that information theory is *assumptions* free, in general there are several assumptions we have to do about the data, for example it is required to assume the data to be stationary, i.e. if a neuron is encoding information about a behavioral variable at the beginning of the experiment, it will do so at the end. Second, because of its probabilistic nature, information theory is applicable regardless of the data type, meaning that we can use it if one of the variables is represented by a binary signal like the case of spikes in a neuron, or if its the continuous variable of speed of an animal in cm/s. Third, information theory can uncover non-linear relations between variables. And finally, all the quantities presented so far are easily scalable to many variables, therefore applicable to many neurons or a neuron and several behavioral variables, etc.

As with anything in life, it does come with its perks and considerations and has to be used with care and a proper understanding of the tools. This is particularly true when dealing with real data, because, although very solid and versatile in its formalism, information theory requires the knowledge of the underlying probability distributions of the variables, which is never really known. Probably the stronger assumption we do when using information theory for real data is that we can get an empirical approximation of the underlying probability distribution, and that it is a good approximation. The bias implied by using empirical probability distributions has been extensively studied and several alternatives for correcting such bias have been proposed [Panzeri et al., 2007, Panzeri and Treves 1995].

Information theory approaches have been traditionally used for studying spiking

trains, and therefore electrophysiological data [Skaggs 1993]. However as we said before, this approach can be used regardless of the nature of the data types, more recently it has been used for analyzing information content and correlations in calcium activity as recorded by 2-photon imaging [Shuman et al., 2020, Stefanini et al., 2020, Rubin et al., 2015, Sheintuch et al., 2017].

1.3.2 Astrocytes and information

In the context of information theory, the first question was whether astrocytes encode information about the position of the animal. To answer this question, mice where trained to run head-fixed in a virtual reality corridor [Figure 1.9a] [Gauthier and Tank 2018]. Using astrocyte-specific expression of the genetically encoded calcium indicator GCaMP6f [Chen; Khakh] together with two-photon functional imaging to capture subcellular calcium dynamics of hippocampal CA1 astrocytes [Figure 1.9b], it was found that that a fraction of astrocytic regions of interest (ROIs) carried significant information about the spatial position of the animal in the virtual track [Figure 1.9c,d]. In this context *significant amount of information* is related to how the mutual information value compares to surrogate distributions of MI values build by temporally shuffling the data (see methods for details). Broadly speaking, this astrocytes show calcium activity that could be interpreted as the glial analogous to the spiking activity of place cells, thus, it is adequate to define the spatial response field of the informative astrocytes and study their characteristics. It was shown that the distribution of field positions covered the entire length of the virtual corridor [Figure 1.9c], suggesting a full map of the environment, done by astrocytes, parallel (or complementary) to that of the neuronal network. Similar to neurons, when exposed to a bidirectional environment, astrocytic ROIs showed significant direction selective spatial modulation in their response field.

Following the discussion from previous sections, it is interesting to see if this coding is intrinsic to astrocytic processes, somas or both. It was found that both cell bodies and processes encoded spatial information and that a larger fraction of somas than processes were modulated by the spatial position of the animal [Figure 1.10a,b]. Unlike neurons, the preferred position of astrocytes was not entirely random. This was observed first because correlation between the calcium activity of pairs of informative ROIs decreased as a function of the pair distance [Figure 1.10c]. And second, because the difference between the field position of the two informative ROIs in a given pair increased as a function of the pair distance within $0 - 40\mu m$ and reached a constant value, indicating that informative calcium signals were coordinated across cells [Figure 1.10d]. Similarly, when looking at the single cell level, the difference between the field position of an informative process and the corresponding somas increased as a function of the process distance from soma [Figure 1.10e], demonstrating that spatial information is differentially encoded in topological distinct locations of the same astrocyte.

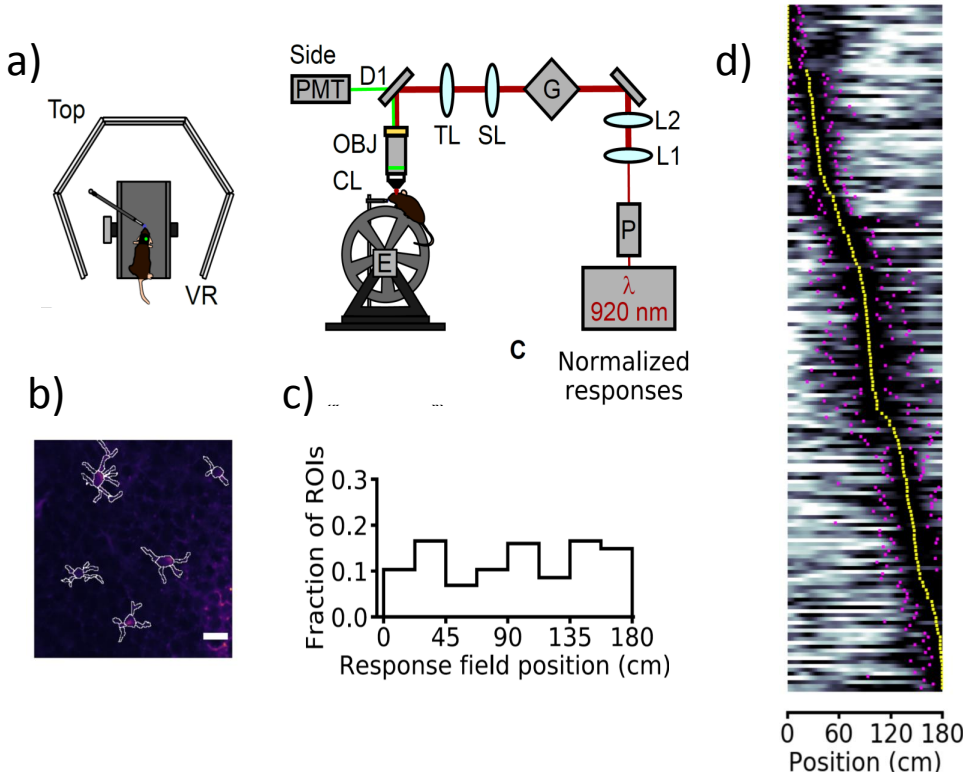

Figure 1.9: Calcium dynamics in astrocytes networks in the hyppocampus encode spatial information. a) Schematics of the experimental setup, head-restrained mice run on a treadmill while navigating a virtual corridor. b) Median projection of GCaMP6f-labeled astrocytes in the CA1 pyramidal layer. Segmented ROIs in white, scale bar is 20 μm. c) Distribution of response field position. d) Normalized astrocytic calcium responses as a function of position for astrocytic ROIs that contain significant amount of spatial information, yellow dots indicate the center position of the response field and magenta dots its width (vertical scale: 50 ROIs)

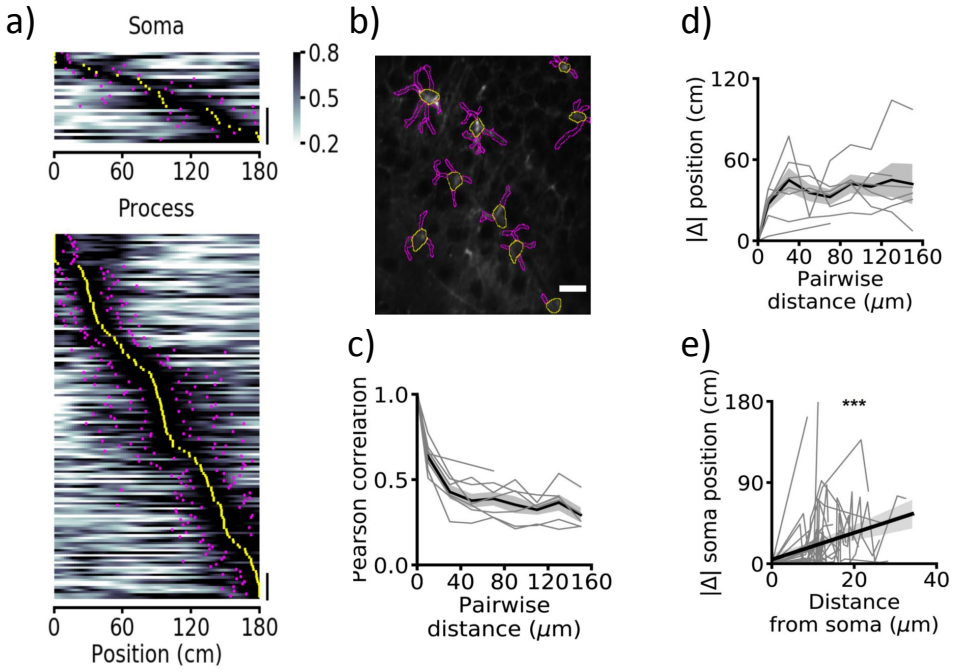

Figure 1.10: Spatial information is encoded differentially in astrocytes somas and processes. a) Normalized astrocytic calcium responses as in 1.9d for ROIs corresponding to somas (top) and processes (bottom) (vertical scale: 10 ROIs). b) Median projection of a t-series displaying GCAMP6f-labeled astrocytes in the CA1 pyramidal layer. ROIs are separated in somas (yellow) and processes (magenta). Pairwise Pearson's correlation (c) and difference between response field position (d) for pairs of astrocytic ROIs across the whole FOV as a function of ROIs pairwise distance. e) Difference in response field position of a process with respect to the field position of the corresponding soma as a function of the process distance from cell soma.

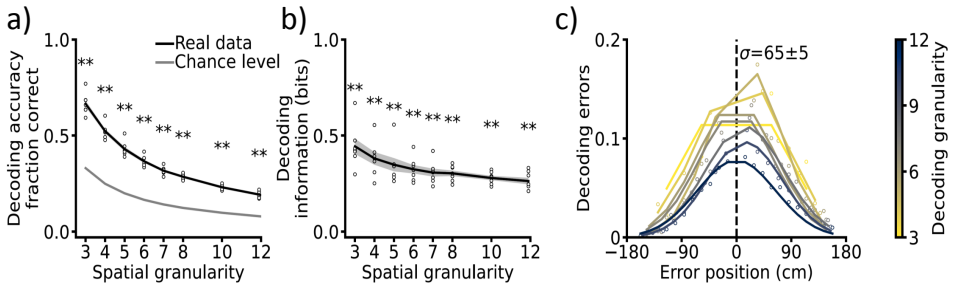

Figure 1.11: Animal's spatial location can be efficiently decoded from astrocytic calcium signals. a) Decoding accuracy as a function of decoding spatial granularity on real (black line) and shuffled (grey line) data. b) Amount of information in bits retrieved by the SVM decoder as a function of granularity. c) Decoding error as a function of the error position within a confusion matrix. Decoding granularity is represented as different lines.

1.3.3 Decoding of position

We've seen that astrocytes encode spatial information in the hyppocampus, and that a complete map (at least in a uni-dimensional virtual track) could be extracted from the network. Meaning that the place fields of all astrocytes observed span the whole space. However, is there sufficient information about space in the astrocytic network to infer the animals position? To answer this question a support vector machine (SVM) was trained to solve the classification problem of decoding mouse's position using single-trial astrocytic calcium signals according to a set of discrete locations. The decoder accuracy, that represents how many times the decoder correctly classify the position of the mouse, was significantly above chance level, regardless of the granularity used in the space domain [Figure 1.11a]. This is important because it means that a downstream neuron (or network) would be able to decode animals position by integrating astrocytic calcium transients information, suggesting the behavioral relevance of it. Decoding spatial information decreased with spatial granularity but, like decoding accuracy, remain significantly above chance for all spatial granularity values used [figure 1.11b]. Misclassifications were more likely to happen among nearby locations across all granularity conditions [figure 1.11c], meaning that decoder errors are not uniformly distributed, suggesting that errors made are *reasonable errors* and not random missclasifications.

Chapter 2

Rational and Aim

Maximum one page, just to state the logical flow in a few sentences and what we gonna do. We know that:

- Astrocytes encode spatial info in Ca2+ activity
- Ca2+ in astrocytes modulates neuronal activity

That brings us to the questions:

- What is the functional role of the Ca2+ signaling in astrocytes in spatial information encoding?
- Does modulation of Ca2+ in astrocytes alter spatial encoding in neurons? how?

To adress this questions we used 1p and 2p imaging + cell specific chemogenetic manipulation in the mouse hippocampus.

Chapter 3

Materials and Methods

3.1 Experimental procedures

3.1.1 Animals

All experiments involving animals were approved by the National Council on Animal Care of the Italian Ministry of Health and carried out in accordance with the guidelines established by the European Communities Council Directive authorization (61/2019-PR). From postnatal days 30, animals were separated from the original cage and group housed (2–5 per cage) in a 12-hours light-dark cycle with *ad libitum* access to food and water. Only animals older than 10 weeks underwent experimental procedures.

3.1.2 AAV injection and chronic hippocampal window surgery

I NEED THE INFO ABOUT THE GCAMP INJECTION IN NEURONS AND CNO gcamp 1/5 and dread 1/8 check with sara

Male C57Bl6/j mice were placed into a stereotaxic apparatus (Stoelting Co, Wood Dale, IL), maintained on a warm platform at 37°C and anesthetized with 2% isoflurane/0.8% oxygen. Before surgery, a bolus of Dexamethasone (4 mg/kg, Dexadreson, MSD Animal Health, Milan, Italy) was provided with an intramuscular injection. A 0.5 mm craniotomy was drilled on the right hemisphere (1.75 mm posterior, 1.35 mm lateral to bregma) after scalp incision. A micropipette loaded with AAV was then lowered into the CA1 region of the hippocampus (1.40 mm deep to bregma). 800 nl of AAV solution was injected at 100 nL/min using a hydraulic injection apparatus driven by a syringe pump (UltraMicroPump, WPI, Sarasota, FL). After viral injection, a stainless-steel screw was positioned on the cranium of the left hemisphere and a chronic hippocampal window was implanted following (D. A. Dombeck, Harvey, et al., 2010, Sheffield and D. Dombeck, 2015). A 3 mm craniotomy centered at coordinates 2.00 mm posterior and 1.80 mm lateral to bregma was opened using a drill and the dura was removed using fine forceps. A blunt needle coupled to a vacuum pump was used to carefully aspirate the cortical tissue overlaying the hippocampus. Exposed tissue was continuously irrigated during aspiration with HEPES-buffered artificial cerebrospinal fluid

(ACSF). Aspiration was interrupted when the thin fibers of the external capsule were visible. After which a cylindrical cannula-based optical window was positioned at the craniotomy touching the external capsule. A thin layer of silicone elastomer (Kwik-Sil, World Precision Instruments, Sarasota, FL) was used to fill and isolate the space between the steel surface of the optical window and the brain tissue. Epoxy glue was used to attach a custom stainless-steel headplate to the skull. Black dental cement was used to secure each component in place. An intraperitoneal bolus of antibiotic (BAYTRIL, Bayer, Germany) was administrated to animals after surgery.

Optical windows consist of stainless-steel cannula segment with thin walls (OD, 3 mm; ID, 2.77 mm; height, 1.50 - 1.60 mm). At one end of the cannula a 3.00 mm diameter round coverslip was attached by means of UV curable optical epoxy (Norland optical adhesive 63, Norland, Cranbury, NJ). Bonding residues and Edges were smoothed with a diamond coated cutter.

3.1.3 Two-photon imaging

Two-photon calcium imaging was performed using a Ultima Investigator or a Ultima II scanheads (Bruker Corporation, Milan, Italy) equipped with raster scanning galvanometers (6 mm or 3 mm) a 16x/0.8 NA objective (Nikon, Milan, Italy), and multi-alkali photomultiplier tubes. For GCaMP6f imaging, the excitation pulsed laser sources were either a Chameleon Ultra or a Chameleon Ultra II, both tuned at 920 nm (80 MHz repetition rate, Coherent, Milan, Italy). Before every experimental session, each FOV was imaged at 740 nm to confirm the expression of DREADD encoding AAV. Laser beams intensity was adjusted using Pockel cells (Conoptics Inc, Danbury, USA). Imaging average power at the objective outlet was $\sim 80 - 110mW$. Fluorescence emission was collected by multi-alkali PMT detectors downstream of appropriate emission filters (525/70 nm for GCaMP6f, 595/50 nm for red reporter fluorophores). Detector signals were digitalized at 12 bits. Here write about the two modalities normal and long Normal Imaging sessions were conducted in raster scanning mode at $\sim$ 3 Hz using 5x optical zooming factor. Images contained 256 pixels x 256 pixels field of view (pixel dwell-time, $4\mu s$; Investigator: pixel size, $0.634\mu m$; Ultima II: pixel size, $0.509\mu m$). Long ...

3.1.4 Animal habituation

After 7-14 days from surgery, animals were subjected to water restriction and delivered 1 ml of water per day. Mouse weight was monitored on a daily basis in order to be maintain between 80 % and 90 % of the *ad libitum* weight through the complete length of the experiments. A minimum of two sessions of "handling" (mouse habituation to the experimenter) was performed two days after water scheduling. Mice were then habituated to the VR setup in the following training sessions. This was achieved by head-restraining the animals for progressively longer periods in the span of approximately one week until reaching 1 hour. In each training/habituation session mice were

simultaneously exposed to the noise generated by the two-photon imaging setup (galvanometer scanning noise, shutter noise), even when no imaging was taking place for noise habituation. Training in the setup was performed until animals felt comfortable enough as to routinely ran along the linear track. On experimental days, mice were head-tethered, and VR session begun after a suitable FOV was identified. 3 to 6 temporal series (750 frames/series, $\sim 250s$), interleaved by 5 minutes breaks, were acquired during ~ 1 hour virtual navigation session. At each imaging session completion, animals were returned to their home cage.

3.1.5 Longitudinal recordings

GET INPUT FROM SARA FOR THE EXPERIMENTAL PROCEDURE OF THE LONGITUDINAL RECORDINGS

3.2 Data acquisition and pre-processing

3.2.1 Virtual reality Linear track

A custom virtual reality (VR) setup was design and implemented using Blender, an open source 3D creation suite (blender.org, version 2.78c). VR was rendered with Blender Game Engine and displayed at a video rate of 60 Hz. The VR environment was a linear corridor with lateral walls depicting three different white textures (vertical lines, mesh and circles) on a black background. Extremes of the corridor were represented as green walls labeled with a black cross. The corridor was 180 cm long and 9 cm wide. The animal was represented in the VR environment with a spherical avatar of radius 2 cm. To simulate touch-interactions with the environment, a touch sensor represented with a rectangular cuboid of dimensions ($x = 5, y = 1, z = 1cm$) was included, protruding the animals avatar parallel to the corridor floor. Composite tiling of five thin-bezel led screens we used to project the avatars point of view in the VR environment (220° horizontal, 80° vertical). Mice could virtually navigate the environment by running on a custom 3D printed wheel (radius 8 cm, width 9 cm). Motion was captured with an optical rotary encoder (Avago AEDB-9140-A14, Broadcom Inc., San Jose, CA), whos signal was converted to a serial mouse input by a single board microcontroller (Arduino Uno R3, Arduino, Ivrea, Italy). Physical motion perform by the animal and measured by input devices was then mapped witha 1:1 correspondence to the virtual environment. To motivate mice to explore and navigate the virtual corridor, a $\sim 4\mu l$ water rewards was delivered upon reaching 115cm. Rewards were delivered through a custom steel lick-port controlled by a solenoid valve (00431960, Christian Bürkert GmbH & Co., Ingelfingen, Germany) and licks were monitored using a capacitive sensor (MTCH102, Microchip Technology Inc., Chandler, AZ). Upon reaching the end of the corridor, animals were teleported back to the beginning of the track to start a new trial. If instead the mouse failed to reach the end of the track within 120 s, the trial was automatically terminated and the animal teleported to the beginning of the track.

After trial termination, either by reaching the end of the track or in terminated runs, animals faced a timeout interval of 5s before the start of the new trial. VR rendering and two-photon imaging acquisition ran on asynchronous clocks. To synchronize both signals, the command signal of the slow galvanometer was used.

3.2.2 Motion correction

Data extracted using 2-photon microscopy produces t-series consisting of sequential *.tiff* images. All images corresponding to a t-series were first concatenated to produce an *.avi* video with no compression. Motion correction was then performed using the *NoRMCorre* algorithm [Pnevmatikakis and Giovannucci, 2017], that corrects non-rigid motion artifacts by estimating motion vectors with subpixel resolution over a set of overlapping patches within the FOV. These estimates are used to infer a smooth motion field within the FOV for each frame. The inferred motion fields are then applied to the original data frames. For *NoRMCorre* correction a patch size of $(48, 48)$ pixels, maximum overlap of $(24, 24)$ pixels between patches, max rigid shift of $(6, 6)$ pixels and a maximum relative shift of each patch with respect to rigid shifts of 3 pixels was used.

Motion correction was applied in two steps, first each t-series was motion corrected individually. Then, all t-series corresponding to the same day and same animal were concatenated and motion corrected again. For longitudinal recordings a third step of motion correction was included. After each day was motion corrected, all days belonging to the same FOV were concatenated and motion corrected again to maximize the correspondence across days. Motion corrected recordings were finally split again and analyzed separately for each day.

3.3 Video Segmentation

To infer neuronal activity, imaging data was first segmented using the algorithm CITE-on (Cell Identification and Trace Extraction online, **cite the biorxiv or publication if ready**). CITE-on is a convolutional neural network-based algorithm for automatic online cell identification, segmentation, identity tracking, and trace extraction in two-photon calcium imaging data. The off-line cell identification suit was used on the median projection of the full length concatenated recordings. By using the median projection of the full motion corrected concatenated recordings, the amount of neurons detected is maximized. In practice, CITE-on implements an image detector based on the publicly available convolutional neural network (CNN) RetinaNet [Lin et al., 2020]. The output of the CNN image detection is a set of boxes tightly surrounding each detected cell soma, from here on called *bounding boxes*. Coordinates and identity of the bounding boxes is saved and used in the following steps. Note that, because the motion correction is performed across t-series, and the median projection is calculated on the full-length recording, the coordinates and identities of the bounding boxes are preserved across frames and t-series and don't need adjustments or tracking across frames.

CITE-on requires an upscaling factor that depends on the ratio between the FOV surface and the average surface of the neuronal somata. This parameter was optimized to obtain the tightest fit of bounding boxes to cell somatas, in all recordings presented in this work this parameter was set to 0.7.

3.4 Longitudinal tracking

In longitudinal recordings video segmentation was applied separately for each day, and cell identities were match a posteriori. To compare sets of bounding boxes, we computed the intersection over union (*iou*) for all pairs of boxes. Pairs with $iou > 0.5$ were considered matching identities, if a box from one set satisfies this condition with more than 1 box from the other set, then the pair with the biggest *iou* was considered as matching identities. Matching procedure was applied between the set of bounding boxes from first day of recording and the second and then between the first and third day of recordings. The intersection between both matching sets are the cells that we considered as **tracked**. All cells that do not have a matching identity between first and second day and/or first and third day are considered as **non tracked** cells.

3.5 Trace extraction

The second step in the inference of neuronal activity consists on extracting calcium traces out of the recordings for the identified cells. This was achieved using the algorithm CaImAn, a popular state-of-the-art method based on Constrained Non-Negative Matrix Factorization (CNMF) [Giovannucci et al., 2019]. We used the bounding boxes generated offline by CITE-On to build binary masks that were used as seeds to initialize the seeded-CNMF algorithm. Seeded-CNMF calculates first the temporal background component of the recording using pixels that were not included in any mask, this background component is later on subtracted from each neuronal factor. It represents the background noise that is shared across all signals including the neuropil activity. Then, the seeded-CNMF algorithm estimates temporal components and spatial footprints, constrained to be non-zero only at the location of the binary masks. Parameters for seeded-CNMF were explored and tuned manually: number of global background components = 2; no merging was performed; number of components per patch $= 4$; expected half size of neurons in pixels $= (7, 7)$; no spatial or temporal subsampling was performed. Finally for each component the $\Delta F/F_0$ was computed with the CaImAn **detrend_df_f** function (see Giovannucci et al., 2019), using the 50^{th} quantile as baseline and a 2000 frames running window to compute quantiles.

The combination of both algorithms was implemented in order to take advantage of the strengths of each, while, at the same time, compensating for their weaknesses. Off-line CITE-on localizes putative neurons considering only anatomical aspect, regardless of their activity profile. CaImAn then refines the segmentation for each

binding box and provides denoised calcium traces. Neither deconvolution nor spike inference were used.

3.6 Event detection

For each component obtained after trace extraction, statistically significant calcium events were detected on the $\Delta F/F$ traces with a modified implementation of the algorithm described in [D. A. Dombeck, Khabbaz, et al., 2007]. Briefly, the standard deviation σ_1 of the signal was computed and points bigger in absolute value than σ_1 were removed from the trace. This procedure automatically excluded large transients. Then, the standard deviation σ_2 of the resulting trace was computed. Fluorescence transients were identified as events that:

i) were bigger in absolute value than 3 σ_2

ii) didn't return within 2 σ_2 before 0.5 s [D. A. Dombeck, Khabbaz, et al., 2007].

These criteria were selected to obtain a false discovery rate $< 5\%$. Here False discovery rate is defined as:

$$FDR = \frac{N_{E_n}}{N_{E_p} + N_{E_n}} \tag{3.1}$$

where N_{E_n} and N_{E_n} are the numbers of identified positive and negative deflections of the $\Delta F/F_0$ trace, respectively. In this way, an **event trace** can be obtained by setting all fluorescent values from the $\Delta F/F_0$ trace that do not belong in a positive event to 0. We call such trace the *event trace*.

3.7 Place Cell detection

3.7.1 Response profiles and response fields

Only instants in which the animal was running at a speed $> 1cm/s$ were considered for the analysis. The virtual corridor was binned using 81 equally spaced bins and the occupancy map was calculated for each animal. The occupancy map represents the total amount of time spent in each spatial bin. Then the activity map was computed for each ROI as the average fluorescence value in each spatial bin. Both the activity and the occupancy map were normalized to sum 1 and convolved with a Gaussian kernel with a width of 3 spatial bins. We then defined the response profile of a ROI (RP) as the ratio of its activity map over the occupancy map. For each RP we defined and computed a response field (RF) as follows:

i) find all local maxima greater than the 25th percentile of the response profile values $C = (c_0, c_1, ..., c_n)$

ii) fit the response profiles as the sum of n parametrized Gaussian functions, with means equal to the elements of C. The amplitud a_i and standard deviations σ_i were constrain to take values $0 \leq a \leq 1$ and $0 \leq \sigma \leq 90cm$ respectively. The

fitting was performed by solving a non-linear least squares problem using the function *curve_fit*, from scipy, www.scipy.org):

$$RP \cong \sum_{c_i \in C} a_i \exp \frac{-(x - c_i)^2}{2\sigma_i^2} \tag{3.2}$$

With constrains

$$\begin{cases} 0 \leq c_i \leq 180 \; \forall \; c_i \in C \\ 0 \leq a_i \leq 1 \; \forall \; a_i \in A \\ 0 \leq \sigma_i \leq 90 \; \forall \; \sigma_i \in S \end{cases} \tag{3.3}$$

iii) the RF was defined as the fitted gaussian with the highest amplitude, and its width as 2 σ_i

$$RF = a_i \exp \frac{-(x - c_i)^2}{2\sigma_i^2} \quad \text{with} \quad i = argmax(A) \tag{3.4}$$

3.7.2 Place cells analysis

Only periods in which the animal running speed was $> 1cm/s$ were used to study the spatial modulation of neuronal cell activity. We defined spatial modulation based on information theory (see section 1.3.1, Shannon, 1948, Quiroga and Panzeri, 2013). We computed the mutual information between position in the linear track P and the neuronal calcium event trace F using equation 1.6

$$I(F \; : \; P) = H(F) + H(P) - H(F, P) \tag{3.5}$$

Where H is the Shannon entropy as defined in equation 1.2:

$$H(X) = -\sum_{x \in X} p(x) \; log_2(p(x)) \tag{3.6}$$

Here $X = (x_0, x_1, ..., x_n)$ represents all possible discrete values of either F or P. And $H(F, P)$ is the joint entropy as defined in equation 1.4. To answer the question of whether a cell carries **significant amount of information** in its calcium activity we compared its mutual information with a surrogate distribution of mutual information values. These values were obtained by calculating the mutual information of surrogate traces that were cyclic permutations of the temporally inverted original trace. The permutations were done by shifting the traces a random amount of time bigger than the 5% of the length of the trace and smaller than the 95%. Importantly, this surrogate method preserves every aspect of the trace, such as auto-correlation, temporal structure, mean value, etc, but destroys the temporal relationship between neuronal activity and position. This procedure was perform 1000 times for each ROI to build the null distribution of mutual information values. A cell whose mutual information value was higher than the 95^{th} percentile of the null distribution was considered a **place cell**.

3.7.3 Bias correction and parameter selection

As metioned in the introduction (see section 1.3.1), using empirical probability distribution as aproximations of the true underlying probability distribution produces biased values of mutual information (MI). The contribution of the bias to the MI value strongly depends in how we choose to bin the variables: higher number of bins better describe the data but produces bins with less counts and therefore worst estimates of their probabilities. To account for this bias we first computed the parameter

$$NsR = log_2(\frac{N_s}{R}) \tag{3.7}$$

with N_s the average number of counts in position bins, and R the number of stimulus bins, that is the amount of steps in which we decide to bin calcium intensities. This parameters gives a quantitative measure of how well we can estimate the probability distribution: the bigger it is, the better or probabilities estimates will be, we consider $NsR = 3$ as a threshold above which the description quality is good. We calculated NsR for each recording for number of intensity bins $r_{bins} = [2, 3, 4, 5, 8, 10, 20]$ and position bins $s_{bins} = [4, 8, 12, 16, 20, 24, 40, 60, 80, 100, 160]$. Then, we calculated the contribution of the bias for each ROI as the mean of the null distribution, using the surrogate distribution described in the previos section. The **unbias value of MI** is thus defined as the MI value calculated as in equation 3.5 minus the bias:

$$MI_{unbiased} = I(F\ :\ P) - \langle I(F_s\ :\ P)\rangle_{surrogates} \tag{3.8}$$

We then calculated the average unbias MI value across ROIs for each combination of numbers of intensity and position bins and their standard deviation, we then splitted this averages in place cells and non-place cells. By doing so we can study the contribution of the bias as a function of the binning of the variables. Higher contribution of the bias will decrease the value of the unbiased MI. At the same time we expect that if the bias is correctly being subtracted then the non place cells would have unbiased MI values close to zero and the place cells positive values. Therefore we selected the appropriate combination of space and intensity binning as the highest number of bins that have a $NsR > 3$ and that maximizes the unbiased MI. This procedure allows comparisons of MI values across recordings, experimental conditions and ROIs. Finally, we performed all the aforementioned procedure for two binning procedures for space: uniform width bins and uniform count bins, the latter yielding a uniform distribution of space occupancy. This last computation serves as a control for the consistency of the unbiased MI values across binning procedures.

3.8 Statistical testing

To compare distribution of independent samples we used the Mann-Whitney U test. For related paired samples we used the Wilcoxon signed-rank test. Both tests are non-parametric, and in both cases the scipy [www.scipy.org] implementation for python was used.

The question whether CNO application had en effect on information content in place cells involves comparisons across conditions for different animals and with different numbers of cells for each recording. The contribution of the animal variability could in principle mask the statistical significance of the condition effect, and the difference in counts brakes the symmetry needed for some standard statistical tests. For these reasons to explore the difference in the information content of cells in both conditions, but excluding the animal variability we fitted a Linear Mixed Effects Model (LMEM) with treatment (CNO or Saline injection) as a fixed effect and animal (or FOV depending on the experimental paradigm) as a random effect. LMEM was fitted using the *lme4* and *lmerTest* and *car* libraries from **R** [R Core Team, 2017], we compare two models, that using the standard nomenclature can be described as

$$MI \sim treatment + (1|animal) \tag{3.9}$$

$$MI \sim treatment + (1 + treatment|animal) \tag{3.10}$$

Equation 3.9 represents a model with one fixed effect and a random intercept for the animal, equation 3.10 adds a random slope to the previous model. To compare both models an ANOVA test was performed, if the more complex model described significantly more variance, then model 3.10 was used. If, on the other hand, there was no significant difference across models, the simpler one (3.9) was prefered. After fitting the model, statistical significance of the fixed effect was tested using a Type II Wald chi-square tests implemented as in the *car::Anova* function.

3.9 Decoding of position from neural activity

3.10 Dimensionality reduction

Chapter 4

Results

4.1 Random Foraging

- Significant decrease in information content in place cells
- Differences in place fields properties (?)

4.2 Open Field

- Significant decrease in information content in place cells
- Differences in place fields properties (?)

4.3 Linear track

- No significant difference in information content
- Difference in place cell and place field properties, maybe as a function of reward and/or position in track

4.4 Population codes

- Decoding of position from neural activity
- Dimensionality reduction

Chapter 5

Discussion

Appendix A

About Appendix

The appendix is usually used to provide some supplementary materials for the publications. For example, some experimental results, network architecture, detailed experimental settings or proving of the theories. You can have more than one appendices to provide the materials for different uses.

Appendix B

Appendix Title Here

Write your Appendix content here.

Appendix C

Appendix Title Here

Write your Appendix content here.

Bibliography

[1] W. R. Adey. "An experimental study of the hippocampal connections of the cingulate cortex in the rabbit". In: *Brain* 74 (1951), pp. 233–247. DOI: https://doi.org/10.1093/brain/74.2.233.

[2] W. R. Adey and M. Meyer. "An experimental study of hippocampal afferent pathways from prefrontal and cingulate areas in the monkey". In: *J. Anat.* 86 (1952), pp. 58–74.

[3] G. Agarwal, I. H. Stevenson, A. Berényi, K. Mizuseki, G. Buzsáki, and F. T. Sommer. "Spatially distributed local fields in the hippocampus encode rat position." In: *Science* 344 (2014), pp. 626–630.

[4] J. Akerboom, N. Carreras Caldéron, L. Tian, S. Wabnig, M. Prigge, J. Tolö, A. Gordus, M. B. Orger, K. E. Severi, J. J. Macklin, R. Patel, S. R. Pulver, T. J. Wardill, E. Fischer, C. Schüler, T. W. Chen, K. S. Sarkisyan, J. S. Marvin, C. I. Bargmann, D. S. Kim, S. Kügler, P. Lagnado L.and Hegemann, A. Gottschalk, E. R. Schreiter, and L. L. Looger. "Genetically encoded calcium indicators for multi-color neural activity imaging and combination with optogenetics." In: *Front. Mol. Neurosci.* 6 (2013), p. 2.

[5] J. Akerboom, T.-W. Chen, T. J. Wardill, L. Tian, J. S. Marvin, S. Mutlu, N. Carreras Caldéron, F. Esposti, B. G. Borghuis, X. R. Sun, A. Gordus, M. B. Orger, R. Portugues, F. Engert, J. J. Macklin, A. Filosa, A. Aggarwal, R. A. Kerr, R. Takagi, S. Kracun, E. Shigetomi, B. S. Khakh, H. Baier, L. Lagnado, S. S.-H. Wang, C. I. Bargmann, B. E. Kimmel, V. Jayaraman, K. Svoboda, D. S. Kim, E. R. Schreiter, and L. L. Looger. "Optimization of a GCaMP Calcium Indicator for Neural Activity Imaging". In: *J. Neurosci.* 40 (2012), pp. 13819–13840.

[6] P. Andersen, T. W. Blackstad, and T. Lomo. "Location and identification of excitatory synapses on hippocampal pyramidal cells". In: *Exp. Brain Res.* 1 (1966), pp. 236–248.

[7] P. Andersen, J. C. Eccles, and Y. Loyning. "Location of postsynaptic inhibitory synapses on hippocampal pyramids". In: *J. Neurophysiol.* 27 (1964), pp. 592–607. DOI: https://doi.org/10.1152/jn.1964.27.4.592.

[8] P. Andersen, J. C. Eccles, and Y. Loyning. "Pathway of postsynaptic inhibition in the hippocampus". In: *J. Neurophysiol.* 27 (1964), pp. 608–619. DOI: https://doi.org/10.1152/jn.1964.27.4.608.

[9] M. Anderson and K. Jeffery. "Heterogeneous modulation of place cell firing by changes in context." In: *Neurosci* 23 (2003), pp. 8827–8835.

[10] L. Bareket-Keren and Y. Hanein. "Carbon nanotube-based multi electrode arrays for neuronal interfacing: progress and prospects." In: *Front. Neural Circuits* 6 (2012), p. 122.

[11] C. Barry, R. Hayman, N. Burgess, and K. Jeffery. "Experience-dependent rescaling of entorhinal grids." In: *Nat. Neurosci.* 10 (2007), pp. 682–684.

[12] C. Barry, C. Lever, R. Hayman, T. Hartley, S. Burton, J. O'Keefe, K. Jeffery, and N. Burgess. "The boundary vector cell model of place cell firing and spatial memory." In: *Rev. Neurosci.* 17 (2006), pp. 71–97.

[13] T. Bjerknes, E. Moser, and M.-B. Moser. "Representation of geometric borders in the developing rat." In: *Neuron* 82 (2014), pp. 71–78.

[14] C. Boccara, F. Sargolini, V. Thoresen, T. Solstad, M. Witter, E. Moser, and M.-B. Moser. "Grid cells in pre- and parasubiculum." In: *Nat. Neurosci.* 13 (2010), pp. 987–994.

[15] S. Bovetti, C. Moretti, and T. Fellin. "Mapping brain circuit function in vivo using two-photon fluorescence microscopy". In: *Microsc. Res. Tech.* 7 (2014), pp. 492–501.

[16] V. Brun, S. T., K. Kjelstrup, M. Fyhn, M. Witter, E. Moser, and M. Moser. "Progressive increase in grid scale from dorsal to ventral medial entorhinal cortex." In: *Hippocampus* 18 (2008), pp. 1200–1212. DOI: 10.1002/hipo.20504..

[17] N. Burgess, J. Donnett, K. Jeffery, and J. O'Keefe. "Robotic and neuronal simulation of the hippocampus and rat navigation." In: *Trans. R. Soc. Lond. B Biol. Sci.* 352 (1997), pp. 1535–1543.

[18] C. Buzsáki, C. A. Anastassiou, and C. Koch. "The origin of extracellular fields and currents– EEG, ECoG, LFP and spikes." In: *Nat. Rev. Neurosci.* 13 (2012), pp. 407–420.

[19] G. Buzsáki. "Theta Oscillations in the Hippocampus". In: *Neuron* 33 (2002), pp. 325–340. DOI: https://doi.org/10.1016/S0896-6273(02)00586-X.

[20] G. Buzsáki and A. Draguhn. "Neuronal Oscillations in Cortical Networks". In: *Science* 304 (2004), pp. 1926–1929. DOI: 10.1126/science.1099745.

[21] K. L. Casey, M. Cuenod, and P. D. Maclean. "Unit analysis of visual input to posterior limbic cortex. II. Intracerebral stimuli". In: *J. Neurophysiol* 28 (1965), pp. 1118–1131. DOI: https://doi.org/10.1152/jn.1965.28.6.1118.

[22] T.-W. Chen, T. J. Wardill, Y. Sun, S. R. Pulver, S. L. Renninger, A. Baohan, E. R. Schreiter, M. B. Kerr R.and Orger, V. Jayaraman, L. L. Looger, K. Svoboda, and D. S. Kim. "Ultrasensitive fluorescent proteins for imaging neuronal activity." In: *Nature* 499 (2013), pp. 295–300.

[23] R. C. Craddock, S. Jbabdi, C.-G. Yan, and J. T. Vogelstein. "Imaging human connectomes at the macroscale". In: *Nat. Methods* 10 (2013), pp. 524–539.

[24] B. G. Cragg. "Afferent connexions of the allocortex". In: *J. Anat.* 99 (1965), pp. 339–357.

[25] B. G. Cragg. "Olfactory and other afferent connections of the hippocampus in the rabbit, rat and cat". In: *Experimental Neurology* 3 (1961), pp. 588–600. DOI: https://doi.org/10.1016/S0014-4886(61)80007-1.

[26] B. G. Cragg. "Responses of the hippocampus to stimulation of the olfactory bulb and of various afferent nerves in five mammals". In: *Experimental Neurology* 2 (1960), pp. 547–572. DOI: https://doi.org/10.1016/0014-4886(60)90031-5.

[27] E. C. Crosby, B. R. DeJonge, and R. Schneider. "Evidence for some of the trends in the phylogenetic development of the vertebrate telencephalon. In Evolution of the Forebrain (eds R. Hassler and H. Stephan)". In: *Georg Thieme Verlag, Stuttgart* (1966), pp. 117–135.

[28] M. Cuenod, K. L. Casey, and P. D. MACLEAN. "Unit analysis of visual input to posterior limbic cortex. I. Photic stimulation". In: *J. Neurophysiol.* 28 (1965), pp. 1101–17. DOI: https://doi.org/10.1152/jn.1965.28.6.1101.

[29] H. Dana, B. Mohar, Y. Sun, S. Narayan, A. Gordus, J. P. Hasseman, G. Tsegaye, G. T. Holt, A. Hu, D. Walpita, R. Patel, J. J. Macklin, C. I. Bargmann, M. B. Ahrens, E. R. Schreiter, V. Jayaraman, L. L. Looger, K. Svoboda, and D. S. Kim. "Sensitive red protein calcium indicators for imaging neural activity". In: *Elife* 5 (2016), pp. 2738–2750.

[30] W. Denk, K. R. Delaney, A. Gelperin, D. Kleinfeld, B. W. Strowbridge, D. W. Tank, and R. Yuste. "Anatomical and functional imaging of neurons using 2-photon laser scanning microscopy." In: *J. Neurosci. Methods* 54 (1994), pp. 151–162.

[31] W. Denk and K. Svoboda. "Photon upmanship: why multiphoton imaging is more than a gimmick." In: *Neuron* 18 (1997), pp. 351–357.

[32] D. A. Dombeck, C. D. Harvey, L. Tian, L. L. Looger, and D. W. Tank. "Functional imaging of hippocampal place cells at cellular resolution during virtual navigation." In: *Nat. Neurosci.* 13 (2010), pp. 1433–1440.

[33] D. A. Dombeck, A. N. Khabbaz, F. Collman, T. L. Adelman, and D. W. Tank. "Imaging Large-Scale Neural Activity with Cellular Resolution in Awake, Mobile Mice". In: *Neuron* 56 (2007), pp. 43–57. DOI: https://doi.org/10.1016/j.neuron.2007.08.003..

[34] T. Fellin, O. Pascual, and P. G. Haydon. "Astrocytes Coordinate Synaptic Networks: Balanced Excitation and Inhibition". In: *Physiology* 21 (2006), pp. 208–215.

[35] Y. Fujita and H. Sakata. "Electrophysiological properties of CA1 and CA2 apical dendrites of rabbit hippocampus". In: *J. Neurophysiol.* 25 (1962), pp. 209–222. DOI: https://doi.org/10.1152/jn.1962.25.2.209.

[36] M. Fyhn, T. Hafting, A. Treves, M. Moser, and E. Moser. "Hippocampal remapping and grid realignment in entorhinal cortex." In: *Nature* 446 (2007), pp. 190–194.

[37] M. Fyhn, S. Molden, M. Witter, E. Moser, and M. Moser. "Spatial representation in the entorhinal cortex." In: *Science* 305 (2004), pp. 1258–1264.

[38] M. Fyhn, T. Solstad, and T. Hafting. "Entorhinal grid cells and the neural basis of navigation." In: *Hippocampal Place Fields* (2008), pp. 237–252.

[39] J. L. Gauthier and D. W. Tank. "A Dedicated Population for Reward Coding in the Hippocampus". In: *Neuron* 99 (2018), pp. 179–193.

[40] A. Giovannucci, J. Friedrich, P. Gunn, J. Kalfon, B. L. Brown, S. A. Koay, J. Taxidis, F. Najafi, J. L. Gauthier, P. Zhou, B. S. Khakh, D. W. Tank, D. B. Chklovskii, and E. A. Pnevmatikakis. "CaImAn an open source tool for scalable calcium imaging data analysis". In: *Elife* 8:e38173 (2019). DOI: 10.7554/eLife.38173.

[41] P. Gloor, C. L. Vera, and L. Sperti. "Electrophysiological studies of hippocampal neurons. I. Configuration and laminar analysis of the 'resting' potential gradient, of the main-transient response to perforant path, fimbrial and mossy fibre volleys, and of 'spontaneous' activity". In: *Electroencephalogr. clin. Neurophysiol.* 15 (1963), pp. 353–378. DOI: https://doi.org/10.1016/0013-4694(63)90060-9.

[42] J. Goodridge and J. Taube. "Preferential use of the landmark navigational system by head direction cells in rats." In: *Behav. Neurosci.* 109 (1995), pp. 49–61.

[43] M. Göppert-Mayer. "Über Elementarakte mit zwei Quantensprüngen". In: *Ann. Phys.* 401 (1931), pp. 273–294.

[44] C. Grienberger and A. Konnerth. "Imaging Calcium in Neurons". In: *Neuron* 73 (2012), pp. 862–885.

[45] R. M. Grieves and K. J. Jeffery. "The representation of space in the brain". In: *Behavioural Processes* 135 (2017), pp. 113–131.

[46] R. Grieves, S. Jedidi-Ayoub, K. Mishchanchuk, A. Liu, S. Renaudineau, and K. J. Jeffery. "The place-cell representation of volumetric space in rats". In: *Nat Commun* 11 (2020), p. 789. DOI: https://doi.org/10.1038/s41467-020-14611-7.

[47] T. Hafting, M. Fyhn, S. Molden, M.-B. Moser, and E. Moser. "Microstructure of a spatial map in the entorhinal cortex." In: *Nature* 436 (2005), pp. 801–806.

[48] T. Hartley, H. Tom, N. Burgess, C. Lever, F. Cacucci, and J. O'Keefe. "Modeling place fields in terms of the cortical inputs to the hippocampus." In: *Hippocampus* 10 (2000), pp. 369–379.

[49] P. Heier. *Fundamental Principles in the structure of the brain: A study of the brain of petromyzon fluviatilis*. Vol. 5. Karger, 1948.

[50] L. Heimer. "Synaptic distribution of centripetal and centrifugal nerve fibres in the olfactory system of the rat. An experimental anatomical study". In: *J. Anat.* 103 (1968), pp. 413–432.

[51] F. Helmchen and W. Denk. "Deep tissue two-photon microscopy". In: *Nat. Methods* 2 (2005), pp. 932–940.

[52] F. Helmchen and J. Waters. "Ca2+ imaging in the mammalian brain in vivo." In: *Eur. J. Pharmacol.* 447 (2002), pp. 119–129.

[53] A. Hill. "First occurrence of hippocampal spatial firing in a new environment". In: *Exp. Neurol.* 62 (1978), pp. 282–297. DOI: https://doi.org/10.1016/0014-4886(78)90058-4.

[54] A. Hjorth-Simonsen. "Some intrinsic connections of the hippocampus in the rat: An experimental analysis". In: *J. Comp. Neurol.* 147.2 (1973), pp. 145–161. DOI: 10.1002/cne.901470202.

[55] A. Hjorth-Simonsen and B. Jeune. "Origin and termination of the hippocampal perforant path in the rat studied by silver impregnation". In: *J. Comp. Neurol.* 144.2 (1972), pp. 215–232. DOI: https://doi.org/10.1002/cne.901440206.

[56] K. Horikawa, Y. Yamada, T. Matsuda, K. Kobayashi, M. Hashimoto, T. Matsuura, A. Miyawaki, T. Michikawa, K. Mikoshiba, and T. Nagai. "Spontaneous network activity visualized by ultrasensitive Ca2+ indicators, yellow Cameleon-Nano". In: *Nat. Methods, vol.* 7 (2010), pp. 729–732.

[57] D. H. Hubel and T. N. Wiesel. "Receptive fields of single neurones in the cat's striate cortex." In: *J. Physiol.* 148 (1959), pp. 574–591.

[58] J. Huxter, N. Burgess, and J. O'Keefe. "Independent rate and temporal coding in hippocampal pyramidal cells". In: *Nature* 425 (2003), pp. 828–832. DOI: https://doi.org/10.1038/nature02058.

[59] M. Jankowski and S. O'Mara. "Dynamics of place, boundary and object encoding in rat anterior claustrum." In: *Front. Behav. Neurosci.* 9 (2015), p. 250.

[60] M. Jankowski, J. Passecker, M. Islam, S. Vann, J. Erichsen, J. Aggleton, and S. O'Mara. "Evidence for spatially-responsive neurons in the rostral thalamus." In: *Front. Behav. Neurosci.* 9 (2015), p. 256.

[61] K. Jeffery. "Integration of the sensory inputs to place cells: what, where, why, and how?" In: *Hippocampus* 17 (2007), pp. 775–783.

[62] J. J. Jun, N. A. Steinmetz, and J. H. Siegle. "Fully integrated silicon probes for high-density recording of neural activity". In: *Nature* 551 (2017), pp. 232–236.

[63] E. R. Kandel, W. A. Spencer, and F. J. Brinley. "Electrophysiology of hippocampal neurons. I. Sequential invasion and synaptic organization". In: *J. Neurophysiol.* 24 (1961), pp. 225–242. DOI: https://doi.org/10.1152/jn.1961.24.3.225.

[64] C. U. A. Kappers, G. C. Huber, and E. C. Crosby. *The comparative anatomy of the nervous system of vertebrates*. Vol. 2. Macmillan, 1936, pp. 1248–1255.

[65] D. I. B. Kerr and B. J. Dennis. "Collateral projection of the lateral olfactory tract to entorhinal cortical areas in the cat". In: *Brain Res.* 36 (1972), pp. 399–403. DOI: https://doi.org/10.1016/0006-8993(72)90743-3.

[66] T. Kim, J. G. McCall, and Y. H. Jung. "Injectable, cellular-scale optoelectronics with applications for wireless optogenetics." In: *Science* 340 (2013), pp. 211–216.

[67] J. Knierim, H. Kudrimoti, and B. McNaughton. "Place cells, head direction cells, and the learning of landmark stability." In: *Neurosci* 15 (1995), pp. 1648–1659.

[68] T. Knöpfel, J. Díez-García, and W. Akemann. "Optical probing of neuronal circuit dynamics: genetically encoded versus classical fluorescent sensors". In: *Trends Neurosci.* 29 (2006), pp. 160–166.

[69] J. E. Krettek and J. L. Price. "Projections from the amygdala to the perirhinal and entorhinal cortices and to the subiculum". In: *Brain Res.* 71 (1974), pp. 150–154. DOI: https://doi.org/10.1016/0006-8993(74)90199-1.

[70] R. M. Lebovitz, M. Dichter, and W. A. Spencer. "Recurrent excitation in the CA3 region of cat hippocampus". In: *Int. J. Neurosci.* 2 (1971), pp. 99–108. DOI: https://doi.org/10.3109/00207457109146996.

[71] G. R. Leichnetz and J. Astruc. "Preliminary evidence for a direct projection of the prefrontal cortex to the hippocampus in the squirrel monkey". In: *Brain Behav. Evol.* 11 (1975), pp. 355–364. DOI: https://doi.org/10.1159/000123645.

[72] C. Lever, S. Burton, A. Jeewajee, J. O'Keefe, and N. Burgess. "Boundary vector cells in the subiculum of the hippocampal formation." In: *J. Neurosci.* 29 (2009), pp. 9771–9777.

[73] T. Y. Lin, P. Goyal, R. Girshick, K. He, and P. Dollar. "Focal Loss for Dense Object Detection". In: *IEEE Trans. Pattern. Anal. Mach. Intell.* 42 (2020), pp. 318–327. DOI: 10.1109/TPAMI.2018.2858826.

[74] L. L. Looger and O. Griesbeck. "Genetically encoded neural activity indicators". In: *Curr. Opin. Neurobiol.* 22 (2012), pp. 18–23.

[75] R. Lorente De Nó. "Studies on the structure of the cerebral cortex. II. Continuation of the study of the ammonic system". In: *Journal für Psychologie und Neurologie* (1934), pp. 113–177.

[76] E. Mankin, G. Diehl, F. Sparks, L. Stefan, and J. Leutgeb. "Hippocampal CA2 activity patterns change over time to a larger extent than between spatial contexts". In: *Neuron* 85 (2015), pp. 190–201. DOI: https://doi.org/10.1016/j.neuron.2014.12.001.

[77] T. W. Margrie, A. Meyer A. H.and Caputi, H. Monyer, M. T. Hasan, A. T. Schaefer, W. Denk, and M. Brecht. "Targeted whole-cell recordings in the mammalian brain in vivo." In: *Neuron* 39 (2003), pp. 911–918.

[78] L. Mariotti, G. Losi, A. Lia, M. Melone, A. Chiavegato, M. Gómez-Gonzalo, M. Sessolo, S. Bovetti, A. Forli, M. Zonta, L. M. Requie, I. Marcon, A. Pugliese, C. Viollet, B. Bettler, T. Fellin, F. Conti, and G. Carmignoto. "Interneuron-specific signaling evokes distinctive somatostatin-mediated responses in adult cortical astrocytes". In: *Nature Communications* 9 (2018). DOI: 10.1038/s41467-017-02642-6.

[79] C. Markus E.J.and Barnes, B. McNaughton, and W. Gladden V.L.and Skaggs. "Spatial information content and reliability of hippocampal CA1 neurons: effects of visual input." In: *Hippocampus* 4 (1994), pp. 410–421.

[80] T. McLardy. "Anticipatory recall deficit after cingulumotomy in rats". In: *Exp. Neurol.* 32 (1971), pp. 141–151. DOI: https://doi.org/10.1016/0014-4886(71)90058-6.

[81] B. McNaughton, C. Barnes, and J. O'Keefe. "The contributions of position, direction, and velocity to single unit activity in the hippocampus of freely-moving rats". In: *Exp. Brain Res.* 52 (1983), pp. 41–49. DOI: https://doi.org/10.1007/BF00237147.

[82] B. McNaughton, F. Battaglia, O. Jensen, E. Moser, and M.-B. Moser. "Path integration and the neural basis of the cognitive map." In: *Nat. Rev. Neurosci.* 7 (2006), pp. 663–678.

[83] A. Miyawaki, J. Llopis, R. Heim, J. M. McCaffery, M. Adams J. A.and Ikura, and R. Y. Tsien. "Fluorescent indicators for Ca2+based on green fluorescent proteins and calmodulin". In: *Nature* 388 (1997), pp. 882–887.

[84] S. Mizumori and J. Williams. "Directionally selective mnemonic properties of neurons in the lateral dorsal nucleus of the thalamus of rats." In: *Neurosci* 13 (1993), pp. 4015–4028.

[85] Y. Mu, D. V. Bennett, M. Rubinov, S. Narayan, C. T. Yang, M. Tanimoto, B. D. Mensh, L. L. Looger, and M. B. Ahrens. "Glia Accumulate Evidence that Actions Are Futile and Suppress Unsuccessful Behavior". In: *Cell* 178 (2019), pp. 27–43.

[86] R. Muller and J. Kubie. "The effects of changes in the environment on the spatial firing of hippocampal complex-spike cells." In: *Neurosci* 7 (1987), pp. 1951–1968.

[87] R. Muller, J. Kubie, and J. Ranck Jr. "Spatial firing patterns of hippocampal complex-spike cells in a fixed environment". In: *J. Neurosci.* https://doi.org/10.1523/JNEUROSCI.07-07-01935.1987 (1987), pp. 1935–1950. DOI: 7.

[88] P. H. J. Nafstad. "An electron microscope study on the termination of the perforant path fibres in the hippocampus and the fascia dentata". In: *Z. Zellforsch. mikrosk. Anal.* 76 (1967), pp. 532–542.

[89] A. Nagy, J. Wu, and K. M. Berland. "Observation volumes and gamma-factors in two-photon fluorescence fluctuation spectroscopy." In: *Biophys. J.* 89 (2005), pp. 2077–2090.

[90] J. O'Keefe and L. Nadel. *The Hippocampus as a Cognitive Map*. Vol. 27. Oxford University Press, 1980.

[91] J. O'Keefe. "Place units in the hippocampus of the freely moving rat". In: *Neurol.* 51 (1976), pp. 78–109. DOI: https://doi.org/10.1016/0014-4886(76)90055-8.

[92] J. O'Keefe and N. Burgess. "Geometric determinants of the place fields of hippocampal neurons." In: *Nature* 381 (1996), pp. 425–428.

[93] J. O'Keefe and D. Conway. "Hippocampal place units in the freely moving rat: why they fire where they fire". In: *Exp. Brain Res* 31 (1978), pp. 573–590.

[94] J. O'Keefe and M. Recce. "Phase relationship between hippocampal place units and the EEG theta rhythm". In: *Hippocampus* 3 (1993), pp. 317–330. DOI: https://doi.org/10.1002/hipo.450030307.

[95] K. Ohki, S. Chung, Y. H. Ch'ng, P. Kara, and R. C. Reid. "Functional imaging with cellular resolution reveals precise micro-architecture in visual cortex." In: *Nature* 433 (2005), pp. 597–603.

[96] M. Ohkura, M. Matsuzaki, H. Kasai, K. Imoto, and J. Nakai. "Genetically Encoded Bright Ca 2+ Probe Applicable for Dynamic Ca 2+ Imaging of Dendritic Spines". In: *Anal. Chem.* 77 (2005), pp. 5861–5869.

[97] M. Ohkura, T. Sasaki, C. Kobayashi, Y. Ikegaya, and J. Nakai. "An Improved Genetically Encoded Red Fluorescent Ca2+ Indicator for Detecting Optically Evoked Action Potentials". In: *PLoS One* 7 (2010), e39933.

[98] A. E. Palmer, Y. Qin, J. G. Park, and J. E. McCombs. "Design and application of genetically encoded biosensors." In: *Trends Biotechnol.* 29 (2011), pp. 144–152.

[99] D. N. Pandya and H. G. J. M. Kupyers. "Cortico-cortical connections in the rhesus monkey". In: *Brain Res.* 13 (1969), pp. 13–36. DOI: https://doi.org/10.1016/0006-8993(69)90141-3.

[100] D. N. Pandya and A. A. Vignolo. "Interhemispheric projections of the parietal lobe in the rhesus monkey". In: *Brain Res.* 15 (1969), p. 49. DOI: https://doi.org/10.1016/0006-8993(69)90309-6.

[101] J. B. Pawley. "Handbook Of Biological Confocal Microscopy." In: *Boston, MA: Springer US* (2006), pp. –.

[102] J. M. Petras. "Connections of the parietal lobe". In: *J. Psychiat. Res.* 8 (1971), pp. 189–201. DOI: https://doi.org/10.1016/B978-0-08-017007-7.50008-2.

[103] E. A. Pnevmatikakis and A. Giovannucci. "NoRMCorre: An online algorithm for piecewise rigid motion correction of calcium imaging data". In: *Journal of Neuroscience Methods* 291 (2017), pp. 83–94. DOI: https://doi.org/10.1016/j.jneumeth.2017.07.031..

[104] T. P. S. Powell, W. M. Cowan, and G. Raisman. "The central olfactory connections". In: *J. Anat.* 99 (1965), pp. 791–813.

[105] J. L. Price and T. P. S. Powell. "Certain observations on the olfactory pathway". In: *Journal of anatomy* 110 (1971), pp. 105–26.

[106] G. Quirk, R. Muller, and J. Kubie. "The firing of hippocampal place cells in the dark depends on the rat's recent experience." In: *Neurosci* 10 (1990), pp. 2008–2017.

[107] R. Q. Quiroga and S. Panzeri. *Principles of Neural Coding*. CRC Press, 2013.

[108] R Core Team. *R: A Language and Environment for Statistical Computing*. R Foundation for Statistical Computing. Vienna, Austria, 2017. URL: https://www.R-project.org/.

[109] G. Raisman, W. M. Cowan, and T. P. S. Powell. "An experimental analysis of the efferent projections of the hippocampus". In: *Brain* 89 (1966), pp. 83–108. DOI: https://doi.org/10.1093/brain/89.1.83.

[110] G. Raisman, W. M. Cowan, and T. P. S. Powell. "The extrinsic afferent, commissural and association fibres of the hippocampus". In: *Brain* 88 (1965), pp. 963–95. DOI: https://doi.org/10.1093/brain/88.5.963.

[111] J. Ranck Jr. "Head direction cells in the deep cell layer of dorsal presubiculum in freely moving rats." In: *In: Buzsaki, G., Vanderwolf, C.H. (Eds.), Electrical Activity of the Archicortex. Hungarian Academy of Sciences, Budapest* (1985), pp. 217–220.

[112] J. Ranck Jr. "Head direction cells in the deep layers of the dorsal presubiculum in freely moving rats." In: *Society for Neuroscience* 10 (1984), p. 599.

[113] F. Raudies, R. Florian, M. Ennio, and M. Hasselmo. "Modeling the influence of optic flow on grid cell firing in the absence of other cues1." In: *J. Comput. Neurosci.* 33 (2012), pp. 475–493.

[114] F. Raudies and M. Hasselmo. "Modeling boundary vector cell firing given optic flow as a cue." In: *PLoS Comput. Biol.* 8 (2012), e1002553.

[115] E. Rolls. "Spatial view cells and the representation of place in the primate hippocampus." In: *Hippocampus* 9 (1999), pp. 467–480.

[116] E. Rolls and S. O'Mara. "View-responsive neurons in the primate hippocampal complex." In: *Hippocampus* 5 (1995), pp. 409–424.

[117] E. Rolls, R. Robertson, and G.-F. Pierre. "Spatial view cells in the primate hippocampus." In: *Neurosci* 9 (1997), pp. 1789–1794.

[118] D. Rowland, Y. Yanovich, and C. Kentros. "A stable hippocampal representation of a space requires its direct experience". In: *Proc. Natl. Acad. Sci. U. S. A.* 108 (2011), pp. 14654–14658.

[119] A. Rubin, N. Geva, L. Sheintuch, and Y. Ziv. "Hippocampal ensemble dynamics timestamp events in long-term memory". In: *eLife* 4:e12247 (2015). DOI: 10.7554/eLife.12247.

[120] E. Save, L. Nerad, and B. Poucet. "Contribution of multiple sensory information to place field stability in hippocampal place cells". In: *Hippocampus* 10 (2000), pp. 64–76.

[121] F. Savelli, D. Yoganarasimha, and J. Knierim. "Influence of boundary removal on the spatial representations of the medial entorhinal cortex." In: *Hippocampus* 18 (2008), pp. 1270–1282.

[122] C. E. Shannon. "A Mathematical Theory of Communication". In: *The Bell System Technical Journal* 27 (1948), pp. 379–423. DOI: 10.1002/j.1538-7305.1948.tb01338.x.

[123] M. Sheffield and D. Dombeck. "Calcium transient prevalence across the dendritic arbour predicts place field properties". In: *Nature* 517 (2015), pp. 200–204. DOI: https://doi.org/10.1038/nature13871.

[124] M. Shein-Idelson, L. Pammer, M. Hemberger, and G. Laurent. "Large-scale mapping of cortical synaptic projections with extracellular electrode arrays". In: *Nat. Methods* 14 (2017), pp. 882–890.

[125] L. Sheintuch, A. Rubin, N. Brande-Eilat, N. Geva, N. Sadeh, O. Pinchasof, and Y. Ziv. "Tracking the Same Neurons across Multiple Days in Ca2+ Imaging Data". In: *Cell Reports* 21 (2017), pp. 1102–1115. DOI: https://doi.org/10.1016/j.celrep.2017.10.013..

[126] D. Shoham, D. E. Glaser, A. Arieli, T. Kenet, C. Wijnbergen, Y. Toledo, R. Hildesheim, and A. Grinvald. "Imaging cortical dynamics at high spatial and temporal resolution with novel blue voltage-sensitive dyes." In: *Neuron* 24 (1999), pp. 791–802.

[127] W. Skaggs, J. Knierim, and B. Kudrimoti H.S. andMcNaughton. "A model of the neural basis of the rat's sense of direction." In: *Adv. Neural Inf. Process. Syst.* 7 (1995), pp. 173–180.

[128] T. Solstad, C. Boccara, E. Kropff, M.-B. Moser, and E. Moser. "Representation of geometric borders in the entorhinal cortex." In: *Science* 322 (2008), pp. 1865–1868.

[129] W. A. Spencer and E. R. Kandel. "Hippocampal neuron responses to selective activation of recurrent collaterals of hippocampofugal axons". In: *Exp. Neurol.* 4 (1961), pp. 149–161. DOI: https://doi.org/10.1016/0014-4886(61)90037-1.

[130] M. E. Spira and A. Hai. "Multi-electrode array technologies for neuroscience and cardiology". In: *Nat. Nanotechnol.* 8 (2013), pp. 83–94.

[131] H. Stensola, T. Stensola, T. Solstad, K. Frøland, M.-B. Moser, and E. Moser. "The entorhinal grid map is discretized." In: *Nature* 492 (2012), pp. 72–78.

[132] C. Stosiek, O. Garaschuk, K. Holthoff, and A. Konnerth. "In vivo two-photon calcium imaging of neuronal networks". In: *Proc. Natl. Acad. Sci. U. S. A.* 100 (2003), pp. 7319–7324.

[133] K. Svoboda and R. Yasuda. "Principles of Two-Photon Excitation Microscopy and Its Applications to Neuroscience". In: *Neuron* 50 (2006), pp. 823–839.

[134] Y. N. Tallini, M. Ohkura, B.-R. Choi, G. Ji, K. Imoto, R. Doran, J. Lee, P. Plan, J. Wilson, H.-B. Xin, A. Sanbe, J. Gulick, J. Mathai, J. Robbins, G. Salama, J. Nakai, and M. I. Kotlikoff. "Imaging cellular signals in the heart in vivo: Cardiac expression of the high-signal Ca2+ indicator GCaMP2". In: *Proc. Natl. Acad. Sci.* 103 (2006), pp. 4753–4758.

[135] J. Taube. "Head direction cells recorded in the anterior thalamic nuclei of freely moving rats." In: *Neurosci* 15 (1995), pp. 70–86.

[136] J. Taube, R. Muller, R. Jr., and J.B. "A quantitative analysis of head-direction cells in the postsubiculum". In: *Society for Neuroscience* 13 (1987), p. 1332.

[137] J. Taube, R. Muller, R. Jr., and J.B. "Head-direction cells recorded from the postsubiculum in freely moving rats: I. Description and quantitative analysis." In: *Neurosci.* 10 (1990), pp. 420–435.

[138] J. Taube, R. J. Muller R.U., and J.B. "Head-direction cells recorded from the postsubiculum in freely moving rats: II. Effects of environmental manipulations." In: *Neurosci.* 10 (1990), pp. 436–447.

[139] L. Thompson and P. Best. "Long-term stability of the place-field activity of single units recorded from the dorsal hippocampus of freely behaving rats". In: *Brain Res.* 509 (1990), pp. 299–308.

[140] L. Tian, S. A. Hires, T. Mao, D. Huber, M. E. Chiappe, S. H. Chalasani, L. Petreanu, J. Akerboom, S. A. McKinney, E. R. Schreiter, C. I. Bargmann, V. Jayaraman, K. Svoboda, and L. L. Looger. "Imaging neural activity in worms, flies and mice with improved GCaMP calcium indicators". In: *Nat. Methods* 6 (2009), pp. 875–881.

[141] K. Uğurbil, J. Xu, E. J. Auerbach, and S. Moeller. "Pushing spatial and temporal resolution for functional and diffusion MRI in the Human Connectome Project". In: *Neuroimage* 80 (2013), pp. 80–104.

[142] D. C. Van Essen, S. M. Smith, D. M. Barch, and T. E. J. Behrens. "The WU-Minn Human Connectome Project: An overview". In: *Neuroimage* 80 (2013), pp. 62–79.

[143] G. W. Van Hoesen, D. N. Pandya, and N. Butters. "Cortical afferents to the entorhinal cortex of the rhesus monkey". In: *Science* 175.4029 (1972), pp. 1471–1473. DOI: 10.1126/science.175.4029.1471.

[144] G. W. Van Hoesen and D. N. Pandya. "Some connections of the entorhinal (area 28) and perirhinal (area 35) cortices of the rhesus monkey III. Efferent connections". In: *Brain Res.* 95 (1975), pp. 39–59. DOI: https://doi.org/10.1016/0006-8993(75)90206-1.

[145] J. Viventi and J. A. Blanco. "Development of high resolution, multiplexed electrode arrays: Opportunities and challenges". In: *Annual International Conference of the IEEE Engineering in Medicine and Biology Society* (2012), pp. 1394–1396.

[146] L. E. White. "Ipsilateral afferents to the hippocampal formation in the albino rat. I. Cingulum projections". In: *J. comp. Neurol.* 113 (1959), pp. 1–41. DOI: https://doi.org/10.1002/cne.901130102.

[147] L. E. White. "Olfactory bulb projections of the rat". In: *Anat. Rec.* 152 (1965), pp. 465–80. DOI: https://doi.org/10.1002/ar.1091520406.

[148] G. Y. Wiederschain. "The Molecular Probes handbook. A guide to fluorescent probes and labeling technologies". In: *Biochem.* 76 (2011), p. 1276.

[149] M. A. Wilson and B. L. McNaughton. "Reactivation of hippocampal ensemble memories during sleep". In: *Science* 265 (1994), pp. 676–679. DOI: 10.1126/science.8036517.

[150] W. Yang and R. Yuste. "In vivo imaging of neural activity". In: *Nat Methods* 14 (2017), pp. 349–359.

[151] M. M. Yartsev and N. Ulanovsky. "Representation of three-dimensional space in the hippocampus of flying bats". In: *Science* 340 (2013), pp. 367–372. DOI: 10.1126/science.1235338.

[152] R. Yoder, B. Clark, J. Brown, M. Lamia, S. Valerio, M. Shinder, and J. Taube. "Both visual and idiothetic cues contribute to head direction cell stability during navigation along complex routes". In: *Neurophysiol.* 105 (2011), pp. 2989–3001.

[153] R. Yoder, B. Clark, and J. Taube. "Origins of landmark encoding in the brain". In: *Trends Neurosci.* 34 (2011), pp. 561–571.

[154] D. Yoganarasimha and J. Knierim. "Coupling between place cells and head direction cells during relative translations and rotations of distal landmarks". In: *Exp. Brain Res* 160 (2005), pp. 344–359.

[155] R. Yuste and L. C. Katz. "Control of postsynaptic Ca2+ influx in developing neocortex by excitatory and inhibitory neurotransmitters." In: *Neuron* 6 (1991), pp. 333–344.

[156] S. Zhang, F. Schönfeld, L. Wiskott, and D. Manahan-Vaughan. "Spatial representations of place cells in darkness are supported by path integration and border information". In: *Front. Behav. Neurosci* 88 (2014), p. 222.

[157] J. Zimmer. "Ipsilateral afferents to the commissural zone of the fascia dentata, demonstrated in decommissurated rats by silver impregnation". In: *J. comp. Neurol.* 142 (1971), pp. 393–416. DOI: https://doi.org/10.1002/cne.901420402.

[158] W. R. Zipfel, R. M. Williams, and W. W. Webb. "Nonlinear magic: multiphoton microscopy in the biosciences." In: *Nat. Biotechnol.* 21 (2003), pp. 1369–1377.

[159] Y. Ziv, L. Burns, E. Cocker, E. Hamel, K. Ghosh, L. Kitch, A. El Gamal, and M. Schnitzer. "Long-term dynamics of CA1 hippocampal place codes". In: *Nat. Neurosci.* 16 (2013), pp. 264–266.

[160] M. Zugaro, E. Tabuchi, and S. Wiener. "Influence of conflicting visual, inertial and substratal cues on head direction cell activity." In: *Exp. Brain Res.* 133 (2000), pp. 198–208.